

Customised fragment libraries for *ab initio* protein structure prediction using a structural alphabet

Surbhi Dhingra^{1,2}, Ramanathan Sowdhamini², Yves-Henri Sanejouand¹,
Frédéric Cadet^{3,4,5,6}, and Bernard Offmann*¹

¹Université de Nantes, CNRS, UFIP, UMR6286, F-44000 Nantes, France

²Computational Approaches to Protein Science (CAPS), National Centre for Biological Sciences (NCBS), Tata Institute for Fundamental Research (TIFR), Bangalore 560-065, India

³University of Paris, BIGR—Biologie Intégrée du Globule Rouge, Inserm, UMR_S1134, Paris F-75015, France

⁴Laboratory of Excellence GR-Ex, Boulevard du Montparnasse, Paris F-75015, France

⁵DSIMB, UMR_S1134, BIGR, Inserm, Faculty of Sciences and Technology, University of La Reunion, Saint-Denis F-97715, France

⁶PEACCEL, Protein Engineering ACCErator, 6 Square Albin Cachot, box 42, 75013 Paris, France

Abstract

Motivation: Computational protein structure prediction has taken over the structural community in past few decades, mostly focusing on the development of Template-Free modelling (TFM) or *ab initio* modelling protocols. Fragment-based assembly (FBA), falls under this category and is by far the most popular approach to solve the spatial arrangements of proteins. FBA approaches usually rely on sequence based profile comparison to generate fragments from a representative structural database. Here we report the use of Protein Blocks (PBs), a structural alphabet (SA) to perform such sequence comparison and to build customised fragment libraries for TFM.

Results: We demonstrate that predicted PB sequences for a query protein can be used to search for high quality fragments that overall cover above 90% of the query. The fragments generated are of minimum length of 11 residues, and fragments that cover more than 30% of the query length were often obtained. Our work shows that PBs can serve as a good way to extract structurally similar fragments from a database of representatives of non-homologous structures and of the proteins that contain less ordered regions.

Availability: Data and scripts are available for download at <https://frama.link/z2wh7rKC>

*corresponding author : bernard.offmann@univ-nantes.fr

Contact: bernard.offmann@univ-nantes.fr

Supplementary information: Supplementary data are available as an annexure to this preprint online.

1 Introduction

A switch has been observed in the field of protein structure prediction (PSP) in the past few decades wherein research is being encouraged in building computational approaches, mostly focusing on Free modelling (FM) or Template-free Modelling (TFM) protocols [1,2]. These approaches are validated through the biannual competition of CASP [3] intending into resolving sequence-structure-function paradigm. The core methodologies around which the free modelling protocols have been developed are fragment-based assembly methods [4–6], threading approaches [7], physics-based methods [8,9] and quite recently machine learning approaches [10]. We have recently reviewed the progress made in the field lately [11].

From these, fragment-based approaches (FBA) have been explored the most for the construction of *ab initio* protein models. Such methodologies rely on assembling structural fragments covering short or long stretches of amino acid sequences from a representative structural database sharing sequence similarity with a query protein. The fundamental behind FBA is that local protein sequence patterns follow a general trend of structural features [12]. This lead to the stipulation that the local conformations for a given protein sequence can be recovered from fragments sharing local sequence similarity with local regions in existing protein structures [13]. FBA proceeds by collecting such local conformations in a fragment library and assembling them to construct potential structural models, mostly by using knowledge-based scoring functions. In short, a number of fragments are generated for each position within the target protein sequence which are then reduced to the best representative, based on different scoring criteria. The fragment lengths vary with the algorithm in question, usually lying within the range of 20 residues [14]. Nonetheless, accurate models have been constructed using fragments as short as 3 residues long [15,16].

In general, fragment based approaches are beneficial in restricting the dimension of conformational search space by limiting the number of fragments used per position. This also serves as a major check point for such algorithms, as they inherently fall behind in exploring alternative conformations for the same sequence [17]. Recently, efforts have been made in overcoming this drawback by redesigning fragment search heuristics [13].

Algorithms have also been developed for fragment mining using non-traditional methods. One such approach is SA-Frag [18], which uses a type of structural alphabet to construct fragment libraries. It builds local profile comparison between target and template structures based on predicted SA sequences. Though, this study placed SA in the converstaion of PSP, it is still not on par with the available sequence counterparts [19]. Yet, this algorithm has left an open space to dig more into the ways different SAs can be exploited for structure prediction.

In the current work, we have evaluated the potential of Protein Blocks (PBs) [20], a structural alphabet, in constructing effective fragment libraries for *ab initio* protein structure modelling. There are several types of structural alphabets (SAs) [21–23] available that focus on clustering protein backbone conformations into a limited set of representative local stretches. Protein Blocks (PBs) emerged with a goal to obtain a good local structure approximation of protein 3D structures when converted into 1D PB sequences

and good prediction of local structures directly from amino acid sequence [20, 24]. This structural alphabet was obtained after an unsupervised clustering using a Self Organizing Map (SOM) [25, 26]. Protein blocks constitute a set of 16 structural prototypes lettered a to p . Each of the PB is 5 residues in length depicting $2(M-1)$ dihedral angles, where M (here $M=5$) is the number of residues constituting the prototype. Using PBs, any protein structure of n residues long can be converted into a PB sequence of length $n-4$. PBs have been shown to approximate on average at 0.42\AA every local conformation of protein structures [27].

Our work makes use of the available applications of PBs. One being translation of 3D protein structure coordinates into a string of readable 1D PB sequence by a procedure commonly named as PB assignment (PBA). Another being the prediction of the probable backbone conformation of a protein sequence in absence of secondary structure and sequence alignment profiles using a knowledge-based scoring function. This algorithm is available in the form of web-based tool called PB-kPRED [28] for the methodology loosely termed as PB prediction (PBP). We have utilised this ability of PBs to approximate protein backbone into mining fragments for *ab initio* modelling of protein structures. The fragments are retained in the form of PB sequence hits from a non-redundant, non-homologous protein database. The quality of fragments are assessed for PB sequences coming from both PB assignment (PBA) and PB prediction (PBP).

The significance of this work has been centered around the idea of extensive conformational space search using a form of structural prototypes as an initial step. PBs are shown to be beneficial in such cases by primarily excavating the template database for local backbone conformations relying primarily on its local conformation.

2 Methods

2.1 Curated Template Database

A database of non-redundant protein structures was set up. Protein chain entries were downloaded from RCSB database (www.rcsb.org) [29] based on the following criteria: (a) Experimental type: X-ray crystallography, (b) Resolution: $\leq 3\text{\AA}$, (c) R-factor: ≤ 0.2 and (d) length of the protein: ≥ 40 residues. These accounted for a total of 23,989 unique protein chains. The hits were further clustered at 30% sequence identity using the KClust algorithm [30], resulting in a total of 7632 protein chains. Additionally, any protein with chain breaks were removed from the clustered sequence set, finally resulting in 5391 unique chains.

PB sequences were assigned for each of these 5391 templates in the final database using an in-house script which alongside generates equivalent DSSP output files and torsion angle files. Secondary structure assignments for each protein chain were congregated using Pdb-tools [31]. All these files along with protein sequence corresponding to each template constituted our curated database.

2.2 Query Dataset

The query dataset used in this work is derived from a previously published publication that focused on building fragment libraries [14]. This dataset is comprised of 43 query protein structures ranging from 59 to 508 residues in length and is provided in Table 1. Each of them is a monomer and has been further categorized into four main SCOP family classes, specifically, all alpha, all beta, alpha plus beta ($\alpha+\beta$) and alpha and beta (α/β).

Table 1: **The query dataset and its characteristics.**

Table summarises the lengths in terms of number of residues and the estimated accuracies of PB predictions as observed for each protein from the query dataset. A PB-kPRED prediction score (last column) of 1 or above has been determined as an indicator of reliable PB sequence prediction [28]. All the proteins in the dataset, except for one, laid above this score cut-off value.

PDB id	SCOP Class	Length (AA)	Length (PDB)	Accuracy (%)	kPred score
1AIL	all- α	73	70	63.6	1.5
1RRO	all- α	108	108	73.1	1.99
1U61	all- α	138	127	65.2	1.43
1SL8	all- α	191	181	77.5	2.23
1QUU	all- α	250	248	63.8	1.51
1T5J	all- α	313	301	65.8	1.61
1PO5	all- α	476	465	Too low	Too low
1MHN	all- β	59	59	69.2	1.79
1TEN	all- β	90	90	72.1	1.94
2G1L	all- β	104	103	70.5	1.86
1IFR	all- β	121	113	67.1	1.68
1BFG	all- β	146	126	83.3	2.53
2FR2	all- β	172	161	70.4	1.85
1EE6	all- β	197	197	79.5	2.33
1UAI	all- β	224	223	71.1	1.9
2C9A	all- β	259	259	68.9	1.77
1O4Y	all- β	288	270	66.1	1.63
1HG8	all- β	349	349	81.9	2.46
1NKG	all- β	508	508	82.7	2.5
1VJW	$\alpha+\beta$	60	59	59.4	1.28
1MWP	$\alpha+\beta$	96	96	89.7	2.86
1GNU	$\alpha+\beta$	117	117	80.6	2.39
1R9H	$\alpha+\beta$	135	118	85.8	2.66
206L	$\alpha+\beta$	164	162	81.9	2.45
2FS3	$\alpha+\beta$	282	280	82.1	2.47
1DZF	$\alpha+\beta$	215	211	85	2.62
1DXJ	$\alpha+\beta$	242	242	74.2	2.1
1MAT	$\alpha+\beta$	264	263	83.9	2.56
1JKS	$\alpha+\beta$	294	280	80.8	2.36
1MC4	$\alpha+\beta$	370	369	77.3	2.22
2FKF	$\alpha+\beta$	462	455	80.3	2.37
1H75	α/β	81	76	74.3	2.06
1IU9	α/β	111	111	68.8	1.77
1E6K	α/β	130	130	77.7	2.24
1P90	α/β	145	123	64.8	1.56
1FTG	α/β	168	168	79.8	2.34
1QCY	α/β	193	193	75.9	2.14
2A14	α/β	263	257	63.4	1.48
1IZZ	α/β	283	276	77.6	2.23
1QUE	α/β	303	303	82.8	2.51
1KRM	α/β	356	349	81.2	2.42
3BSG	α/β	414	404	77.2	2.21
1PGN	α/β	482	473	72.7	1.98

Each query structure was further transformed into a PB sequence using two concurrent procedures:

- PB-Assignment (PBA) procedure. In this case the query PB sequence is retrieved directly from the PDB coordinate files using an in-house PB assignment script, following the basic principle of PB generation, i.e conversion of 3D information into 1D sequence as described before [20]. In short, the dihedral angles of all constitutive overlapping pentapeptides from a query are used to classify each of them in one of the 16 PB classes a to p . Secondary structure representations for the target protein were here obtained using DSSP assignment protocol [32].
- PB-Prediction (PBP) procedure. Here the potential query PB sequences were manually predicted using the PB-kPRED web tool [28]. This step was done to account for the loss of information endured due to probabilistic estimation of PBs per position for a given sequence. PB-kPRED features a prediction quality criterion in the form of a prediction score and a standardized accuracy percentile. Generally, a score of < 1 concludes unreliable prediction. The prediction accuracies and kPRED scores for the query dataset are shown in the Table 1. Secondary structure representations for the target protein were here estimated by the secondary structure prediction tool Psipred [33].

2.3 Fragment Mining

A procedure was setup to mine non-homologous fragments from the curated template database. To avoid any bias in the benchmarking of our method, the primary step of the procedure involved looking for sequence homologs in the template database. Any template protein sharing more than 30% sequence identity with any the query protein sequence was considered for removal: pairwise sequence identity was calculated for each query against the entire curated template database using Needleman and Wunch global alignment algorithm [34]. Any hit sharing more than the defined sequence identity cut-off with the target sequence was removed from the template database for that run. A local PB alignment tool, PB-Align [35] was used to generate alignment hits for minimum length of 7 PBs corresponding to 11 amino acid long sequence stretches. PB alignment hits whereby the query PB sequence was identical to the template fragment were collected as viable fragments, since it should correspond to identical backbone conformations. Further fragment quality assessment was performed on all identical hits using the criteria discussed below. The overall process of fragment generation is summarised in Figure 1.

2.4 Fragment Quality Assessment

Two sets of experiments were conducted to assess the quality of fragments generated for each protein of the query dataset: one corresponds to real life scenario and considered PB sequences obtained from the PBP procedure, and the other corresponds to the positive control which considered PB sequences obtained with the PBA procedure.

For every position, fragment quality was assessed by fitting fragment hits over query coordinates for that position using the McLachlan algorithm for rapid comparison of protein structures [36] implemented in the ProFit program (www.bioinf.org.uk/software/profit/). This criterion gauged the "precision" of the procedure in generating viable fragments. Here, precision is defined as the number of fragments lying under a $rmsd$ of 2\AA divided

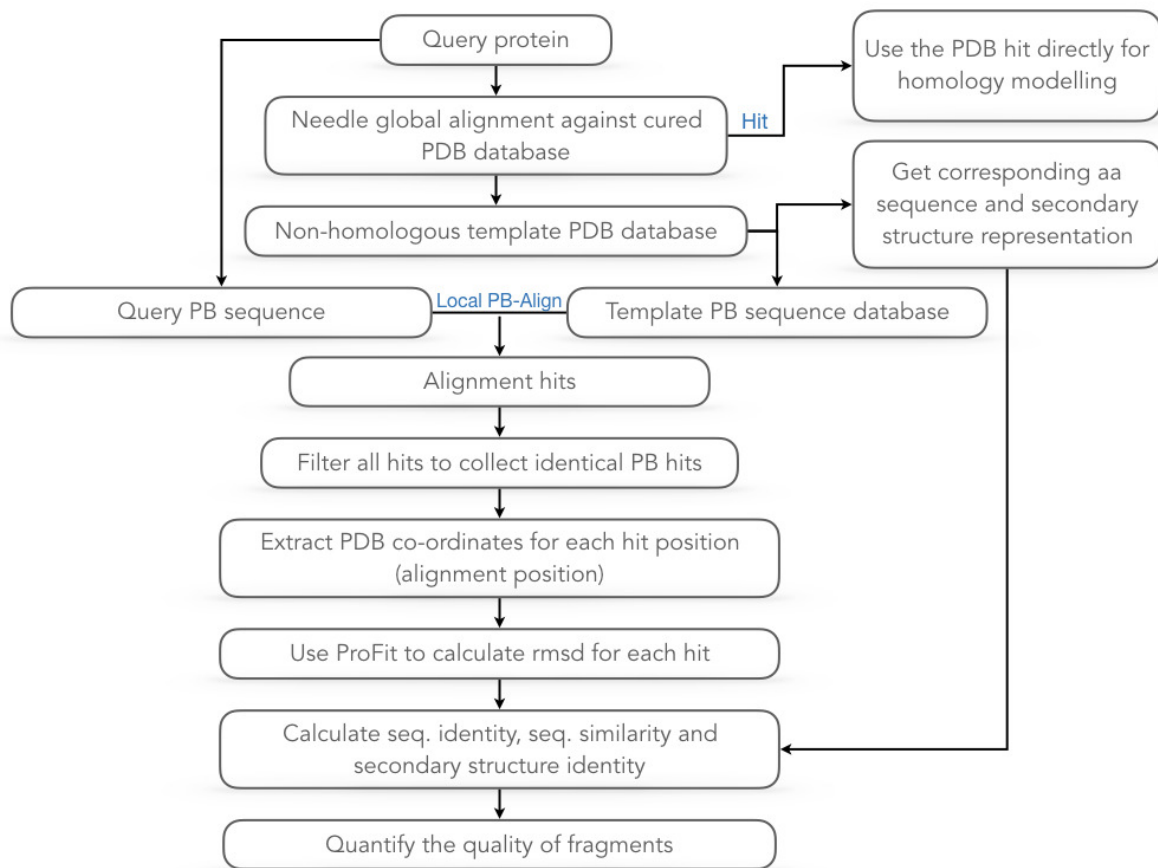


Figure 1: **Fragment Generation Procedure.** Shown is a schematic representation of the general flow of fragment generation carried out using protein blocks as primary source. Local PB alignment between query and template PB sequence effectuates fragments of minimum length of 11 amino acid residues. The alignment hits are then analysed based on several criteria to procure the quality of the generated fragments.

by the total number of fragments generated for the query protein. The second main criterion that was examined was coverage which was defined as the number of positions in the query sequence for which at least one fragment was obtained by the fragment mining procedure. Other assessment criteria that were tested include calculation of amino acid sequence identity and similarity and secondary structure identity between each fragment hit against the target sequence.

3 Results

3.1 Template database

The final template database consisted of 5391 protein chains clustered at $< 30\%$ sequence identity and having a resolution of $< 3\text{\AA}$. The examination of the secondary structural elements distribution in the curated database showed that it is populated with 44.76% helices, 27.82% of strands and 27.42% coils and loops. In terms of PBs, the database corresponded to 29.9% PB *m* the central part of alpha-helices, 19.13% PB *d* the central part of a strand and 51% of other PBs (or coils), which approximated to the general protein secondary structure distribution (regular and irregular) [24].

Our database contained templates from 10 out of 12 SCOP representative classes, with the majority being associated to the 4 main SCOP classes. Out of 5391 proteins, 1962 found no corresponding SCOP hit. This might be due to delay in synchronisation of structural annotation data across platforms.

3.2 Fragment mining and generation

The fragment generation procedure is illustrated in Figure 1. Any protein from our curated template database that could have been a probable sequence homologue with a protein from our query dataset was excluded on the fly from the template database. In this scenario, any template sharing $>30\%$ identity with the query sequence was considered as a *homologue*. This ensures the premises of Free Modelling and the legitimacy of our pipeline in picking up good fragments in absence of sequence homologues.

An average of $\sim 60\text{k}$ hits were generated by local PB-align for each query sequence with least being 34,655 for 1AIL and maximum being 86,866 for 1HG8. The fragments were further filtered on the basis of PB sequence identity. All the PB hits that were 100% identical to the query PB sequence, whether this was assigned (PBA) or predicted (PBP), were chosen as best representative fragments. This functioned as a preliminary filtering step by limiting the fragment search area to the best PB fit. In doing so, the average number of fragments reduced to $\sim 13\text{k}$ hits per query without significantly affecting the overall coverage. The lowest number of identical hits was documented for query protein 1EE6 with 3761 hits and maximum for 1MWP with 21732 hits. Detailed counts of the total hits before and after filtering are provided in Supplementary Tables 1 and 2 for PBA and PBP respectively.

As seen in the Figure 2, the maximum number of fragments laid below 15 residues in length. This remained the case for all the query proteins, whatever their total length. The longest fragments obtained were 65 and 61 residues long for PBA and PBP schemes respectively.

The overall effectiveness of the fragment generating pipeline was judged on the basis of *rmsd* calculations and coverage attained by the fragments for all the queries. Figure 3 shows an overview of *rmsd* distribution as observed in all the cases for both PBA and

PBP schemes. It is clear from the graph that most of the fragment hits lie below the *rmsd* cut-off of 2.5Å which approximates to 85% of the generated fragments.

A barplot depicting the overall percent of sequence space covered (coverage) for each query protein is shown in Figure 4. Higher coverage was observed in case of PBA with an average of 96.5% in comparison to PBP with an average of 93.9%. For 6 cases, PBP gave better percentage coverage than PBA cases. Protein queries belonging to all- β SCOP

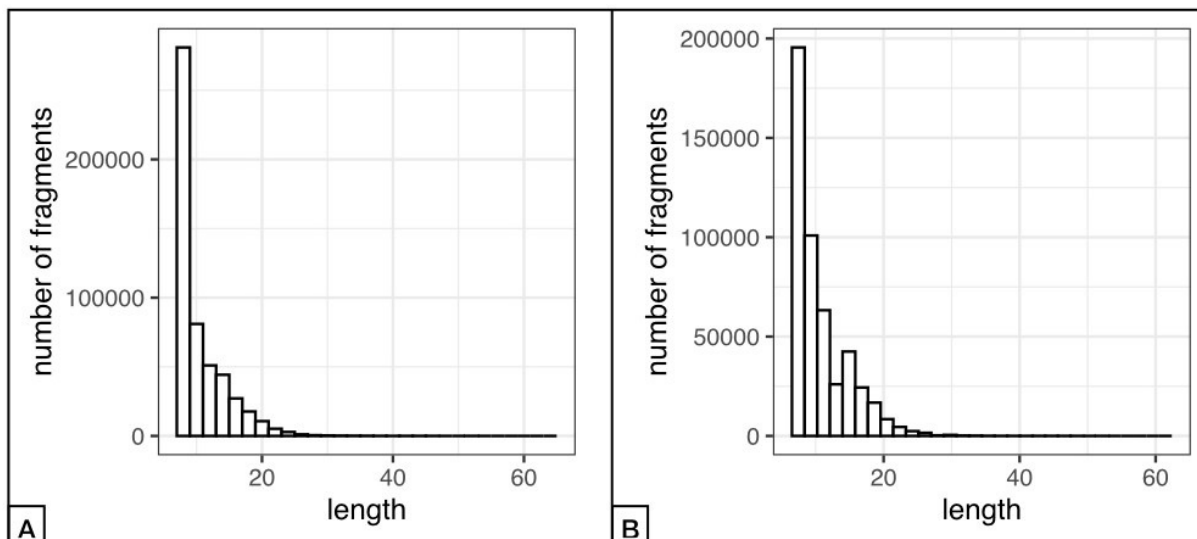


Figure 2: **Fragment length distribution : Protein Block Assignment (left) and Protein Block Prediction (right)**. In both the cases maximum number of fragments are lying at the assigned minimum fragment length of 7 residues. The histogram is plotted for fragment length against number of fragments generated. There is an exponential drop in number of fragments generated with the increase in fragment length.

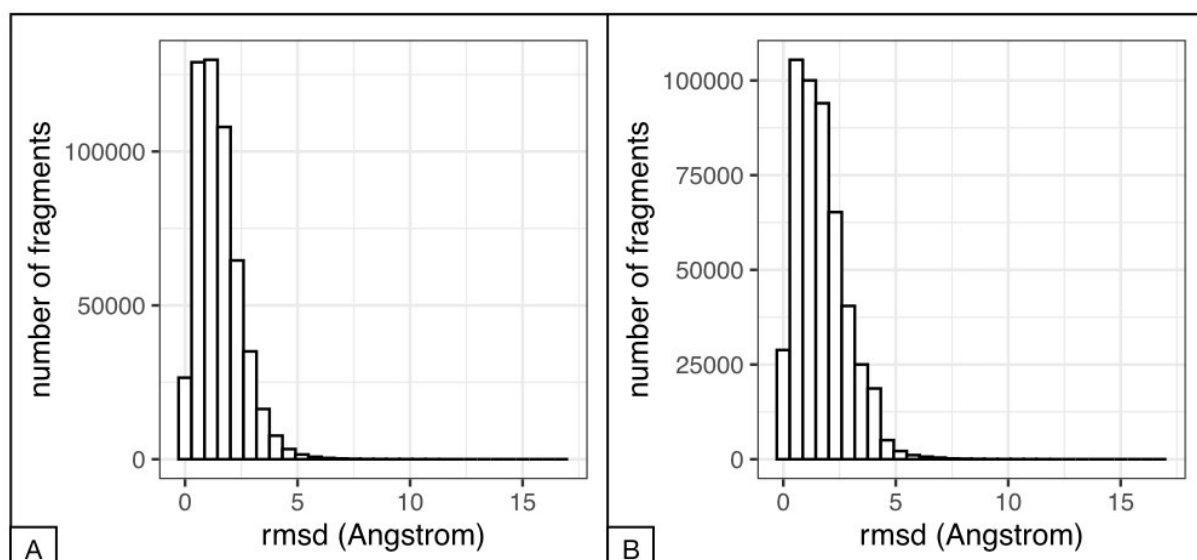


Figure 3: **Rmsd distribution : Protein Block Assignment (left) and Protein Block Prediction (right)**. The graph is plotted for total number of fragments generated from all the queries in test dataset against the rmsd observed when these fragments are fitted over original query structure. For both the cases of PB production, maximum number of fragments lie below the rmsd cut-off value of 2.5 Å.

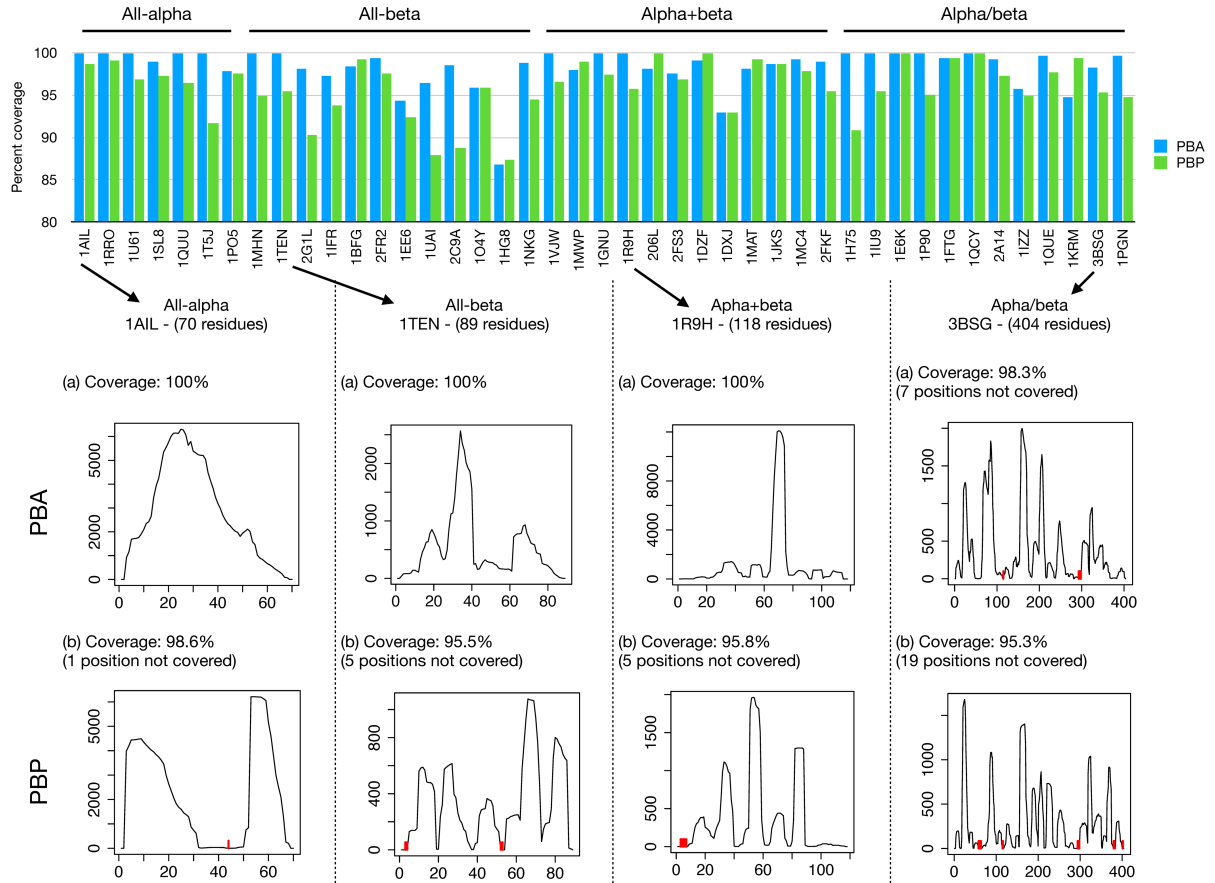


Figure 4: **Coverage analysis of fragments generated.** *Top:* barplot showing, for each query protein from our query dataset, the percentage of positions covered by a fragment (y axis is from 80-100% and x-axis are the labels for the PDB codes of the queries). Results obtained with PBA and PBP procedures are shown in blue and green respectively. Query proteins are grouped according to their SCOP classes. The queries with lowest coverage belongs to SCOP β class. *Bottom:* detailed coverage results illustrated for 4 query examples for both PBA and PBP schemes. The x-axis represents the residue positions and the y-axis is the raw count of the number of fragments that covered each of the positions. Positions not covered by any fragment are shown in red on the plots.

class showed lowest percentage coverage when compared to queries from the other three main SCOP classes.

The number of hits observed per position also varied between the two cases for each query. This is illustrated in Figure 4 for four examples drawn one from each SCOP class and in Supplementary Figures 1 and 2 for all the queries. Both coverages for PBA and PBP schemes are shown. In many queries, the coverage was heterogenous with some positions that were covered by a low number of fragments and some positions with a high number of hits. This is well illustrated by the spikes in the number of hits along the query protein length. These highly covered stretches mostly correspond to regions with canonical secondary structures stretches. Noteworthily, on average, lower number of hits were observed per position in case of PBP without affecting the overall coverage of the query sequence. This can be explained by the loss of accuracy procured in case of PB predictions (Figure 4 and Supplementary Figures 1 and 2).

3.3 Assessment of fragment quality

The quality assessment was primarily done by fitting fragment hits onto the original structures using a protein structure least square fitting program. It was measured in terms of precision, which is defined as the percentage of number of hits lying under a given *rmsd* cut-off. Table 2 summaries the precision percentage values obtained for each SCOP class analysed in the current work at three *rmsd* cut-off values. An overall precision of 75.4% and 64.3% was calculated for PBA and PBP respectively at the *rmsd* cut-off of 2Å. Least precision was quantified for SCOP class all-beta reaching up to 71.8% and 47.7% for PBA and PBP schemes respectively. Rest of the classes had higher precision levels lying above 65% collectively. With more stringent *rmsd* cut-off values, the precision dropped.

Table 2: Precision of the pipeline in generating fragments at three *rmsd* cut-off values. The table describes the precision gained by the fragment generation pipeline as seen at three different *rmsd* cutoff values of 1.5Å, 2Å and 2.5Å. It also compares the precision that could be achieved at the best case scenario of exact PB sequence (PBA) when compared to predicted PB sequences (PBP). At the *rmsd* cut-off of 2Å, the pipeline is able to retain an average precision of 64%. Lowest precision has been noted for hits belonging to SCOP class all- β proteins.

SCOP Class	PBA scheme (<i>rmsd</i> Å)			PBP scheme (<i>rmsd</i> Å)		
	≤ 1.5	≤ 2.0	≤ 2.5	≤ 1.5	≤ 2.0	≤ 2.5
all α	66.2	80.8	89.9	51.7	67.5	80.0
all β	46.1	71.8	84.5	28.9	47.7	64.4
$\alpha + \beta$	55.1	73.6	85.4	51.4	68.7	80.3
α / β	61.3	75.4	85.6	58.1	73.4	83.9
Average	57.2	75.4	86.4	47.5	64.3	77.2

Amino acid sequence identity and similarity and secondary structure identity were calculated for all fragments against corresponding position in the query sequence. Figure 5 depicts their overall distributions. Note that amino acid sequence identity distribution is dominated by fragments sharing no identity (0%) with the query sequence. On the other hand, an increase in sequence similarity is observed in the plots, but the graphs are still skewed towards low values, indicating low similarity correspondence between query and template amino acid sequences. This was not the case for secondary structure identity: the distribution shifted towards right with maximum hits reaching up to 100% identity. This attributes to the nature of PB sequences which depict 1D sequences associated to the local backbone conformation, thus indicating towards it being an objective criteria for assessing and qualifying fragments.

Interestingly, 40% of the fragments lying under *rmsd* of 2Å didn't share any sequence identity with the query sequence and 90% shared less than 37.50% sequence identity. This result could be appreciated as it aligns with the specifics of template database being non-homologous, thereby lowering the chances of finding the exact same amino acid sequence hit altogether for the variable lengths of fragments extracted. The aggregation was consistent in both PBA and PBP schemes: 50% of the data shared <25% sequence similarity with query sequence with 75% of the data reaching \sim 36% sequence similarities in case of PBP. Noteworthily, an average secondary structure identity of 85% was noted for fragments lying below the 2Å mark with most being 100% identical for both PBA and PBP.

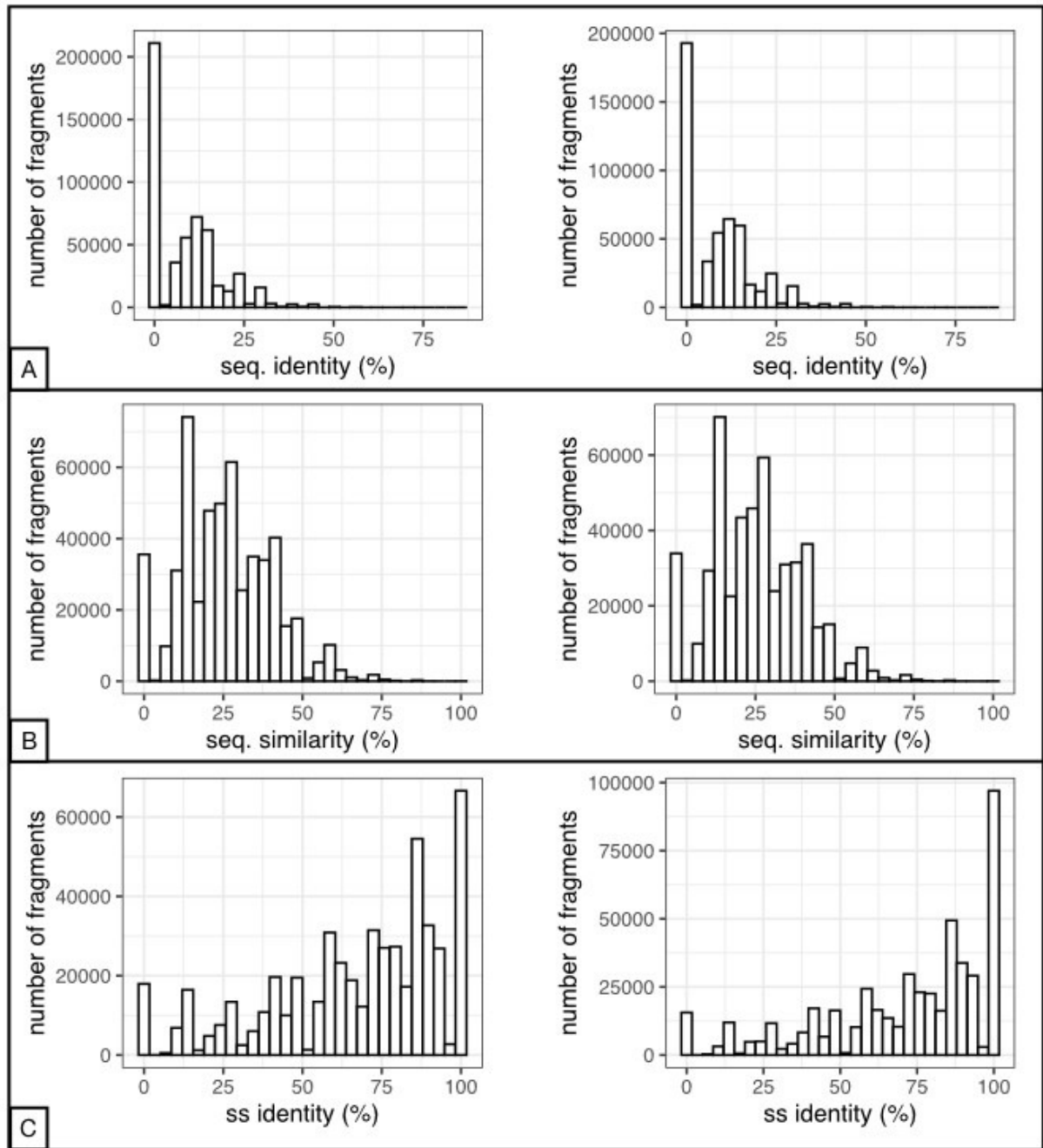


Figure 5: **Qualitative analysis of fragment hits.**

The graphs above exhibit the distribution of sequence identity, sequence similarity and secondary structure identity as observed in case of fragments generated for two working cases of PB generation, PBA (left) and PBP (right). [A] The graphs shows the distribution of amino acid sequence identity. [B] Amino acid sequence similarity distribution as observed between query sequences from test dataset and the fragments generated by the pipeline. [C] Secondary structure identity shared between query sequences and fragments generated by the pipeline. Both the cases of PB generation, i.e PBA and PBP, follow a similar trend of identity and similarity distribution.)

A ROC curve analysis (Figure 6) performed for the aforementioned elements against *rmsd* (2Å) confirmed that secondary structure identity criteria was indeed the best amongst the three tested criteria for prioritising fragments. The sensitivity and specificity curves for individual SCOP classes are further detailed in Supplementary Figures 2.

A visual inspection of the fragments in Pymol [37] shows that the global fold of the target structures can be retained by the fragments. Sample of this visualization is illustrated in Figure 7.

4 Discussion

In the current paper, protein blocks have shown to hold a potential for effective fragment mining towards the goal of *ab initio* protein structure prediction. The work concludes that a huge amount of good quality fragments can be extracted from structural database represented in the form of PBs in absence of sequence homology. It is a very simple pipeline that mimics amino acid sequence pairwise alignment algorithms to detect, thanks to PB alignment, local structural hits within the working database of structural templates. This shifts the fragment-based approaches from relying on amino acid sequence to directly accessing structural patterns from a curated database. Huge pool of structural stretches of varying lengths were recovered for each query in the dataset equating to congregated fragments data. This importantly included loop regions that connect regular secondary structures.

The primary requirement of the study was to effectively depict amino acid sequence

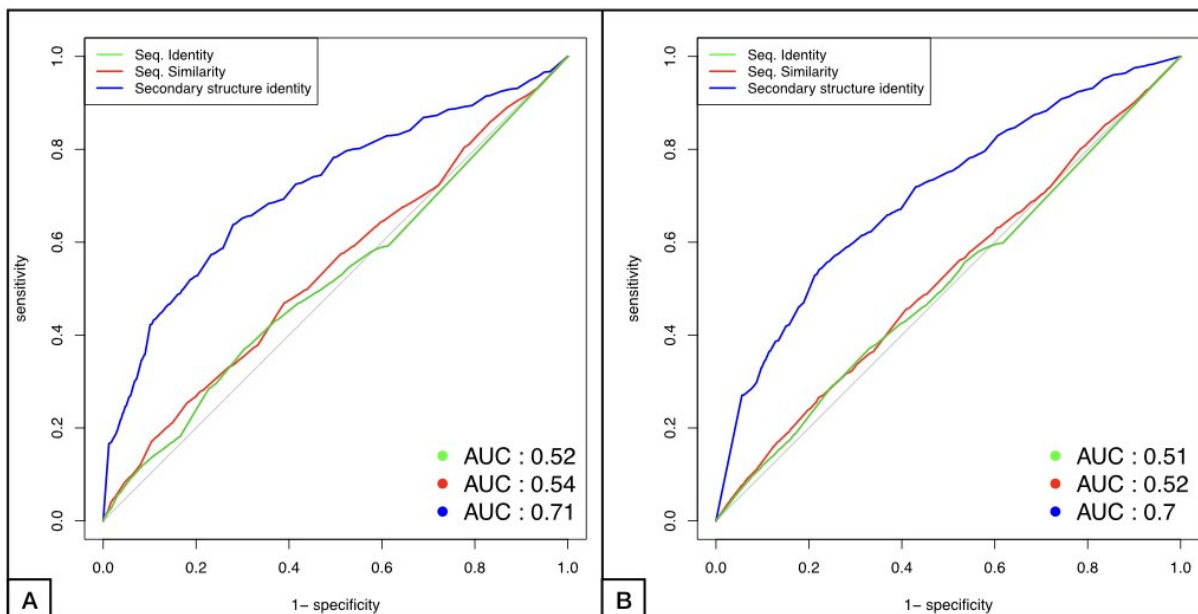


Figure 6: **ROC analysis using three objective criteria.**

A) and B) represent results for PBA and PBP schemes respectively. For all the fragments lying below the *rmsd* cut-off of 2Å, ROC curve was plotted to visualize effective criteria for choosing viable fragments. The three criteria are: (i) amino acid sequence identity (green), (ii) amino acid sequence similarity (red) and (iii) secondary structure identity (blue). Sequence identity and similarity lie on the mark of 50% depicting no direct correlation with the quality of the fragments generated. SS identity, on the other hand, has an AUC of approximately 70%, ensuring its role in recuperating good fragments.

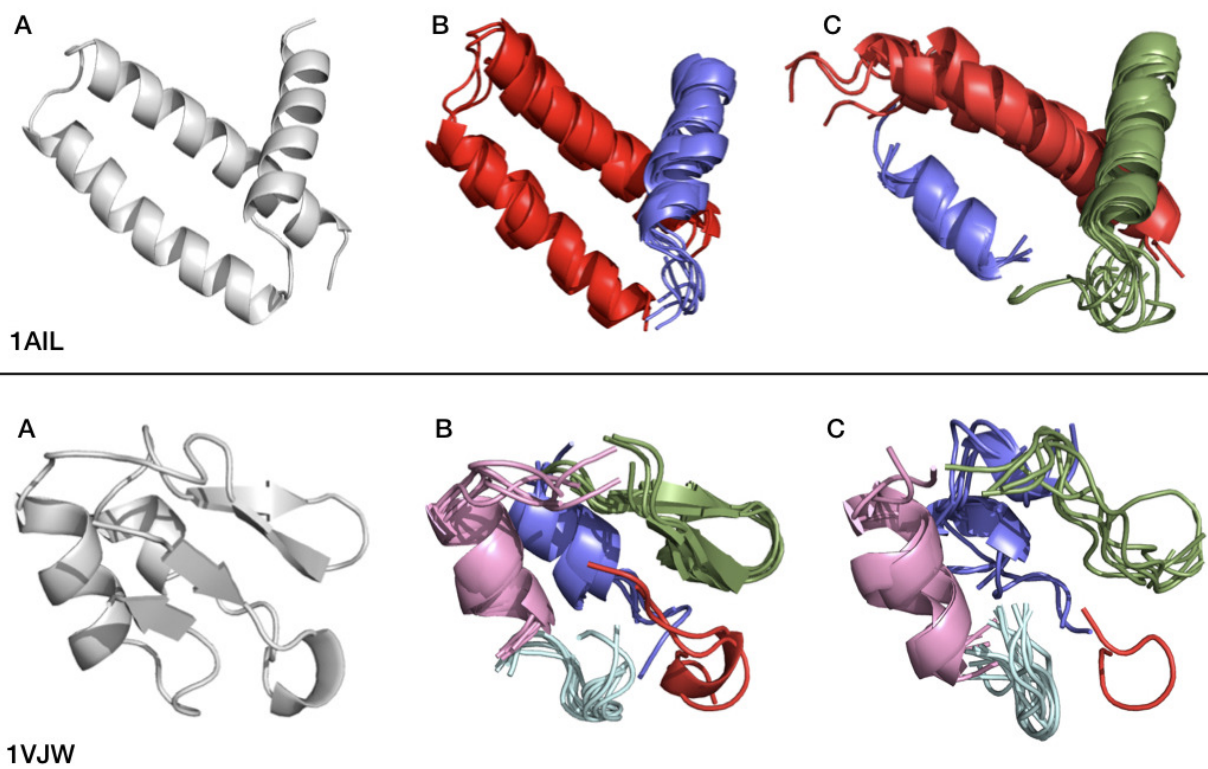


Figure 7: **Superimposition of fragments generated onto the original query structures.**

The figure shows the original structure of two queries from the test dataset, namely, 1AIL and 1VJW, along with the clusters of best fragments retained for each. Here, (A) is original structure, (B) is the fragments clusters obtained for PBA scheme and (C) is the fragments clusters obtained for PBP scheme.

into reliable PB sequences while retaining the probable local conformation. It was attained by using a previous work done in our group ([28]) for optimizing possible PB per position for each overlapping pentapeptide within a protein sequence (PB-kPRED webserver). The calculated PB prediction scores for all the target proteins from the dataset were above the standardized threshold, with an exception of one (1PO5). The average accuracy of PB-prediction was noted to be 74.98 % for 42 out of 43 targets in the dataset, which was ample to guide valid fragment picking through the pipeline.

Prior to running fragment extraction protocol, it was insisted upon abiding by the constraints of free modelling approaches to avoid biasing the aftermath of fragment quality assessment. In line with it, any potential homologous template sequence was removed from the curated database as a preliminary step. This consequently produced personalised database for each query sequence. This step also ensured objectivity of the pipeline when inspecting the quality of fragments generated through PB-predicted sequences.

From our analysis, it was noted that fragments generated via this pipeline show no correspondence between amino acid sequence identity or similarity and *rmsd*. On the other hand, secondary structure juxtaposition between the template fragments with the predicted secondary structure for the query showed excellent relevance. The data unanimously favoured secondary structure identity comparison, with a large proportion of fragments that hit 100% secondary structure identity. A similar trend was observed when examining the correlation between *rmsd* and secondary structure identity. Higher secondary structure identity corresponded to lower *rmsd* between template fragments and query (data not shown). This is not surprising since PB itself is a representation of the backbone.

The quality of fragments was measured by fitting fragment coordinates onto original structure and was termed here as "precision". This was evaluated for the 4 main SCOP classes, all agreeing with the cumulative results of the pipeline. Significant discrepancies were noted for class all-beta. Here the accuracy of fragment prediction did not reach the mark of other classes. In general, it has been noticed that alpha folds are easier to map back to than beta strands. This was even seen in the current study where the 'all-beta' queries showed overall higher *rmsd* and more scattered secondary structure identity distribution.

The pipeline was tested against the best possible case of PB representation, i.e PB assignment (PBA) and was compared to real life scenario of approximating PB sequence for the given query through PB prediction (PBP). This accounted for the effects of missed data (information) on the process of fragment picking. Our results shown that the overall quality of fragments retained in case of PBP was not compromised.

The quality of fragments was judged on the basis of two common criteria used in earlier work done on fragment library generation pipelines, i.e precision and coverage. Though, the overall efficiency of our pipeline is on a par with other algorithms available like HHFrag and NNMake that report precision of 62.16% and 38.17% respectively [14]. Higher precision of HHFRAG can be attributed to the presence of sequence homologues in the working database [14] which is not the case here. SAfrag, another SA based fragment mining pipeline, has shown a precision of 86.7% [18]. Their SAfrag strategy was built on the grounds similar to HHFrag and uses HMM-based profile-profile comparison to generate fragment hits. It makes use of structural alphabets that describe 27 states. The pipeline carried out profile comparison based on the pre-segregated or partitioned query sequence segments into sub-sets of varying lengths of 6 to 27 residues. These sub-sets were then used to search for similar profiles within the established structural data banks. It has to be noted that SAfrag used two types of structural data banks: PDB25 and

PDB50 for fragment generation. The higher precision and coverage of this algorithm can be attributed to the grounds that during the fragment search they accept the inclusion of the target structure as well as data coming from structural homologs as well in their template database.

The coverage attained in our work lies on the higher range when compared to these other algorithms (HHFrag - $71\% \pm 13$, NNMake - $\sim 92\%$) [14]: lowest coverage was observed in case of all-beta class, while the rest showed a coverage of above 90%. It was also observed that fragments predominantly belonging to SS class of alpha-helix were predicted more accurately than other secondary structure classes.

The primary results produced by our procedure are promising and can be worked on towards its further refinement. Improvements could be achieved by both repopulating the core of our curated structural database to increase the variability in fragment selection and the PB-PENTAPEPT database underlying PB-kPRED. The latter is expected to increase the accuracy of PB prediction which in turn will influence the precision and coverage. Another way of improving the precision could be decreasing the minimum length of the fragment, which was not done initially as the coverage achieved was still good.

The procedure that was developed in this study drifts from conventional fragment mining approaches by using PB sequences instead of amino acid sequences for producing fragment libraries. We have also challenged the idea of relying on sequence similarity for identifying reasonable fragments. It further discriminates from SA-Frag for it focused on building pairwise PB sequence alignment profiles between the target protein and templates from a database without any imposed length constraints and without taking advantage of sequence homologues or distantly related proteins.

5 Conclusion

Our work shows that structural alphabets are useful to find fragments for prediction of protein structures in template-free modelling approaches. SAs are indeed more liberating when compared to amino acids sequence based fragment libraries due to their potential in accessing a more expanded conformational space. This aids in broadening the search space without losing the potential to capture the native fold of the target protein. They can successfully be implemented in foraging potential structural homologues for proteins sharing otherwise low or no amino acid sequence similarity. We show here that fragments covering the entire length of small proteins can be readily generated easing the task for structure prediction protocols.

Since, PBs are local conformations represented in the form of 1D sequence, the tenacity of pulling fragments sharing similar fold is higher when compared to the possibility of that happening with amino acid sequence comparison. Longer fragments representing entire domains can be extracted using the protocol. In general, PBs hold a promising step towards protein structure prediction protocols using the local conformations as a starting point.

Acknowledgements

The authors thank Dr Alexandre G. de Brevern and Prof Narayanaswamy Srinivasan for fruitful discussions on this work.

Funding

This work has been supported by the Conseil Régional de La Réunion and Fonds Social Européen in the form of a PhD scholarship to SD under tier number 234275, convention number DIREN/20161451. BO is thankful to Conseil Régional Pays de la Loire for support in the framework of GRIOTE grant.

Competing interests

F.C. is linked to Peaccel. SD, RS, YHS and BO declare no competing interests.

References

- [1] Kevin J Maurice. SSThread: Template-free protein structure prediction by threading pairs of contacting secondary structures followed by assembly of overlapping pairs. *Journal of Computational Chemistry*, 35(8):644–656, 2014.
- [2] Bee Yin Khor, Gee Jun Tye, Theam Soon Lim, and Yee Siew Choong. General overview on structure prediction of twilight-zone proteins. *Theoretical Biology and Medical Modelling*, 12(1):15, 2015.
- [3] John Moult, Jan T Pedersen, Richard Judson, and Krzysztof Fidelis. A large-scale experiment to assess protein structure prediction methods. *Proteins: Structure, Function, and Bioinformatics*, 23(3):ii–iv, 1995.
- [4] Carol A Rohl, Charlie EM Strauss, Kira MS Misura, and David Baker. Protein structure prediction using Rosetta. In *Methods in Enzymology*, volume 383, pages 66–93. Elsevier, 2004.
- [5] Yang Zhang, Adrian K Arakaki, and Jeffrey Skolnick. TASSER: an automated method for the prediction of protein tertiary structures in CASP6. *Proteins: Structure, Function, and Bioinformatics*, 61(S7):91–98, 2005.
- [6] Dong Xu and Yang Zhang. Ab initio protein structure assembly using continuous structure fragments and optimized knowledge-based force field. *Proteins: Structure, Function, and Bioinformatics*, 80(7):1715–1735, 2012.
- [7] Ambrish Roy, Alper Kucukural, and Yang Zhang. I-TASSER: a unified platform for automated protein structure and function prediction. *Nature Protocols*, 5(4):725, 2010.
- [8] JL Klepeis and CA Floudas. ASTRO-FOLD: a combinatorial and global optimization framework for ab initio prediction of three-dimensional structures of proteins from the amino acid sequence. *Biophysical Journal*, 85(4):2119–2146, 2003.
- [9] S Ołdziej, C Czaplewski, A Liwo, M Chinchio, M Nancias, J A Vila, M Khalili, Y A Arnautova, A Jagielska, M Makowski, H D Schafroth, R Kaźmierkiewicz, D R Ripoll, J Pillardy, J A Saunders, Y K Kang, K D Gibson, and H A Scheraga. Physics-based protein-structure prediction using a hierarchical protocol based on the UNRES force field: Assessment in two blind tests. *Proceedings of the National Academy of Sciences*, 102(21):7547–7552, 2005.

- [10] Mohammed AlQuraishi. AlphaFold at CASP13. *Bioinformatics*, 35(22):4862–4865, 2019.
- [11] Surbhi Dhingra, Ramanathan Sowdhamini, Frédéric Cadet, and Bernard Offmann. A glance into the evolution of template-free protein structure prediction methodologies. *arXiv preprint arXiv:2002.06616*, 2020.
- [12] Kim T Simons, Charles Kooperberg, Enoch Huang, and David Baker. Assembly of protein tertiary structures from fragments with similar local sequences using simulated annealing and bayesian scoring functions. *Journal of Molecular Biology*, 268(1):209–225, 1997.
- [13] Shaun M Kandathil, Mario Garza-Fabre, Julia Handl, and Simon C Lovell. Improved fragment-based protein structure prediction by redesign of search heuristics. *Scientific Reports*, 8(1):1–14, 2018.
- [14] Saulo HP de Oliveira, Jiye Shi, and Charlotte M Deane. Building a better fragment library for *de novo* protein structure prediction. *PloS One*, 10(4), 2015.
- [15] Richard Bonneau, Jerry Tsai, Ingo Ruczinski, Dylan Chivian, Carol Rohl, Charlie EM Strauss, and David Baker. Rosetta in CASP4: progress in ab initio protein structure prediction. *Proteins: Structure, Function, and Bioinformatics*, 45(S5):119–126, 2001.
- [16] Dominik Gront, Daniel W Kulp, Robert M Vernon, Charlie EM Strauss, and David Baker. Generalized fragment picking in Rosetta: design, protocols and applications. *PloS One*, 6(8), 2011.
- [17] Shaun M Kandathil, Julia Handl, and Simon C Lovell. Toward a detailed understanding of search trajectories in fragment assembly approaches to protein structure prediction. *Proteins: Structure, Function, and Bioinformatics*, 84(4):411–426, 2016.
- [18] Yimin Shen, Géraldine Picord, Frédéric Guyon, and Pierre Tuffery. Detecting protein candidate fragments using a structural alphabet profile comparison approach. *PloS one*, 8(11), 2013.
- [19] Jad Abbass and Jean-Christophe Nebel. Customised fragments libraries for protein structure prediction based on structural class annotations. *BMC Bioinformatics*, 16(1):136, 2015.
- [20] Alexandre G. de Brevern, Catherine Etchebest, and Serge Hazout. Bayesian probabilistic approach for predicting backbone structures in terms of protein blocks. *Proteins: Structure, Function, and Bioinformatics*, 41(3):271–287, 2000.
- [21] Ron Unger, David Harel, Scot Wherland, and Joel L Sussman. A 3D building blocks approach to analyzing and predicting structure of proteins. *Proteins: Structure, Function, and Bioinformatics*, 5(4):355–373, 1989.
- [22] Anne-Cloude Camproux, Romain Gautier, and Pierre Tuffery. A hidden Markov model derived structural alphabet for proteins. *Journal of Molecular Biology*, 339(3):591–605, 2004.
- [23] Shuai Cheng Li, Dongbo Bu, Xin Gao, Jinbo Xu, and Ming Li. Designing succinct structural alphabets. *Bioinformatics*, 24(13):i182–i189, 2008.

- [24] Agnel Praveen Joseph, Garima Agarwal, Swapnil Mahajan, Jean-Christophe Gelly, Lakshmiapuram S Swapna, Bernard Offmann, Frédéric Cadet, Aurélie Bornot, Manoj Tyagi, Hélène Valadié, Bohdan Schneider, Catherine Etchebest, Narayanaswamy Srinivasan, and Alexandre G De Brevern. A short survey on protein blocks. *Biophysical Reviews*, 2(3):137–145, 2010.
- [25] Teuvo Kohonen. Self-organized formation of topologically correct feature maps. *Biological Cybernetics*, 43(1):59–69, 1982.
- [26] T. Kohonen, M. R. Schroeder, and T. S. Huang, editors. *Self-Organizing Maps*. Springer-Verlag, Berlin, Heidelberg, 3rd edition, 2001.
- [27] Alexandre G de Brevern. New assessment of a structural alphabet. *In Silico Biology*, 5(3):283–289, 2005.
- [28] Iyanar Vetrivel, Swapnil Mahajan, Manoj Tyagi, Lionel Hoffmann, Yves-Henri Sanejouand, Narayanaswamy Srinivasan, Alexandre G De Brevern, Frederic Cadet, and Bernard Offmann. Knowledge-based prediction of protein backbone conformation using a structural alphabet. *PloS One*, 12(11), 2017.
- [29] Helen M Berman, John Westbrook, Zukang Feng, Gary Gilliland, Talapady N Bhat, Helge Weissig, Ilya N Shindyalov, and Philip E Bourne. The Protein Data Bank. *Nucleic Acids Research*, 28(1):235–242, 2000.
- [30] Maria Hauser, Christian E Mayer, and Johannes Söding. kClust: fast and sensitive clustering of large protein sequence databases. *BMC Bioinformatics*, 14(1):248, 2013.
- [31] João PGLM Rodrigues, João MC Teixeira, Mikaël Trellet, and Alexandre MJJ Bonvin. Pdb-tools: a swiss army knife for molecular structures. *F1000Research*, 7, 2018.
- [32] Wolfgang Kabsch and Christian Sander. Dictionary of protein secondary structure: pattern recognition of hydrogen-bonded and geometrical features. *Biopolymers*, 22(12):2577–2637, 1983.
- [33] Liam J McGuffin, Kevin Bryson, and David T Jones. The PSIPRED protein structure prediction server. *Bioinformatics*, 16(4):404–405, 2000.
- [34] Saul B Needleman and Christian D Wunsch. A general method applicable to the search for similarities in the amino acid sequence of two proteins. *Journal of Molecular Biology*, 48(3):443–453, 1970.
- [35] Manoj Tyagi, Venkataraman S Gowri, Narayanaswamy Srinivasan, Alexandre G de Brevern, and Bernard Offmann. A substitution matrix for structural alphabet based on structural alignment of homologous proteins and its applications. *Proteins: Structure, Function, and Bioinformatics*, 65(1):32–39, 2006.
- [36] Andrew D McLachlan. Rapid comparison of protein structures. *Acta Crystallographica Section A*, 38(6):871–873, 1982.
- [37] Warren L DeLano et al. Pymol: An open-source molecular graphics tool. *CCP4 Newsletter on Protein Crystallography*, 40(1):82–92, 2002.

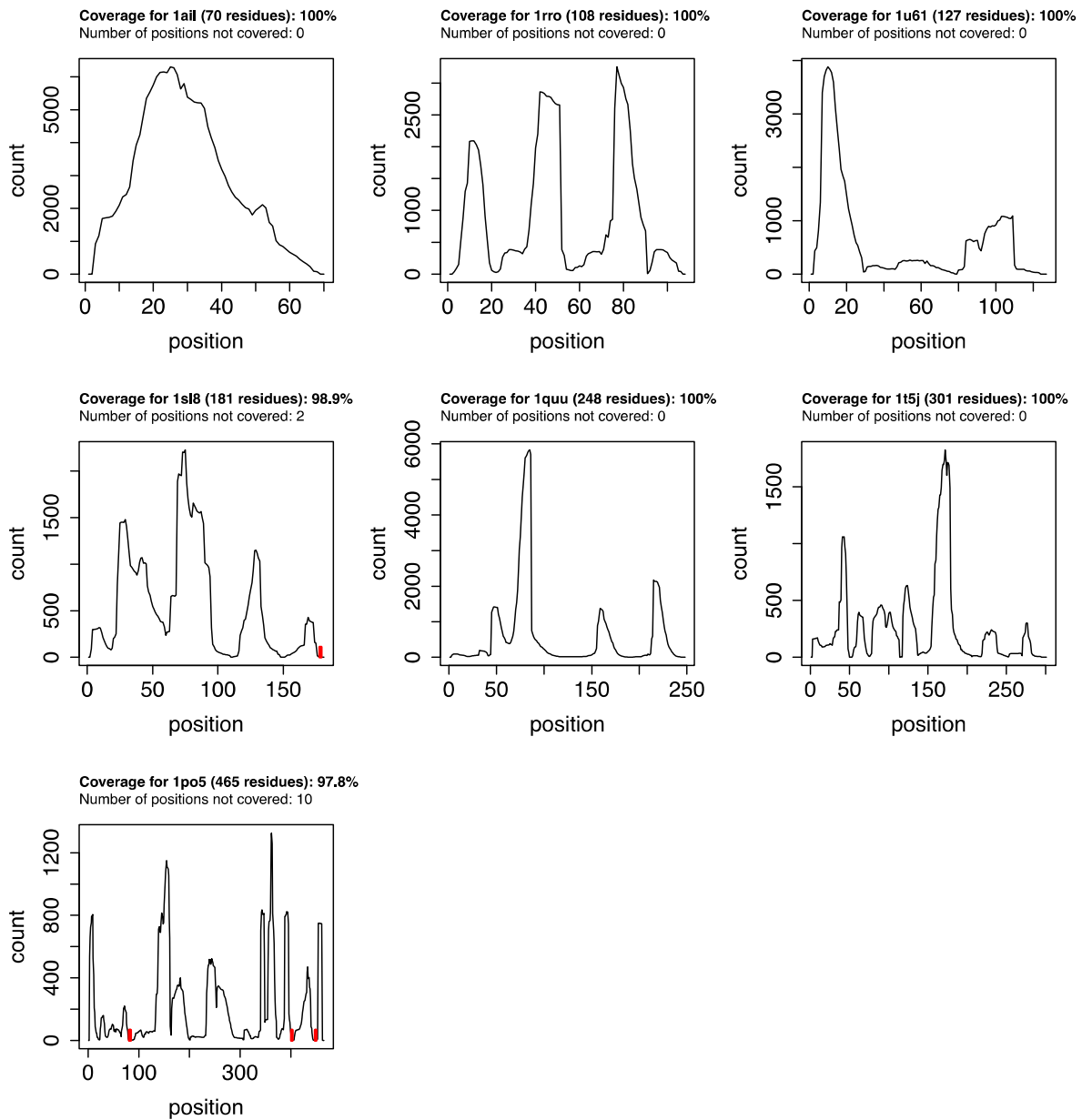
Supplementary Figures and Tables

Supplementary Figures 1. Coverage density plots.

The plots under this heading show the distribution of the number of fragments per position. The analysis has been performed for both treatment of the query proteins: (1) Protein Block Assignment (PBA) and (2) Protein Block Prediction (PBP). The graphs are further classified into section : (a) SCOP Class – all α , (b) SCOP Class – all β , (c) SCOP Class - $\alpha + \beta$ and (d) SCOP Class - α/β . The percentage of coverage for each test protein is marked above the plot. Along with it the positions for each protein with no fragment hits are marked in red and the number of residues with no hits is also shown above each graph.

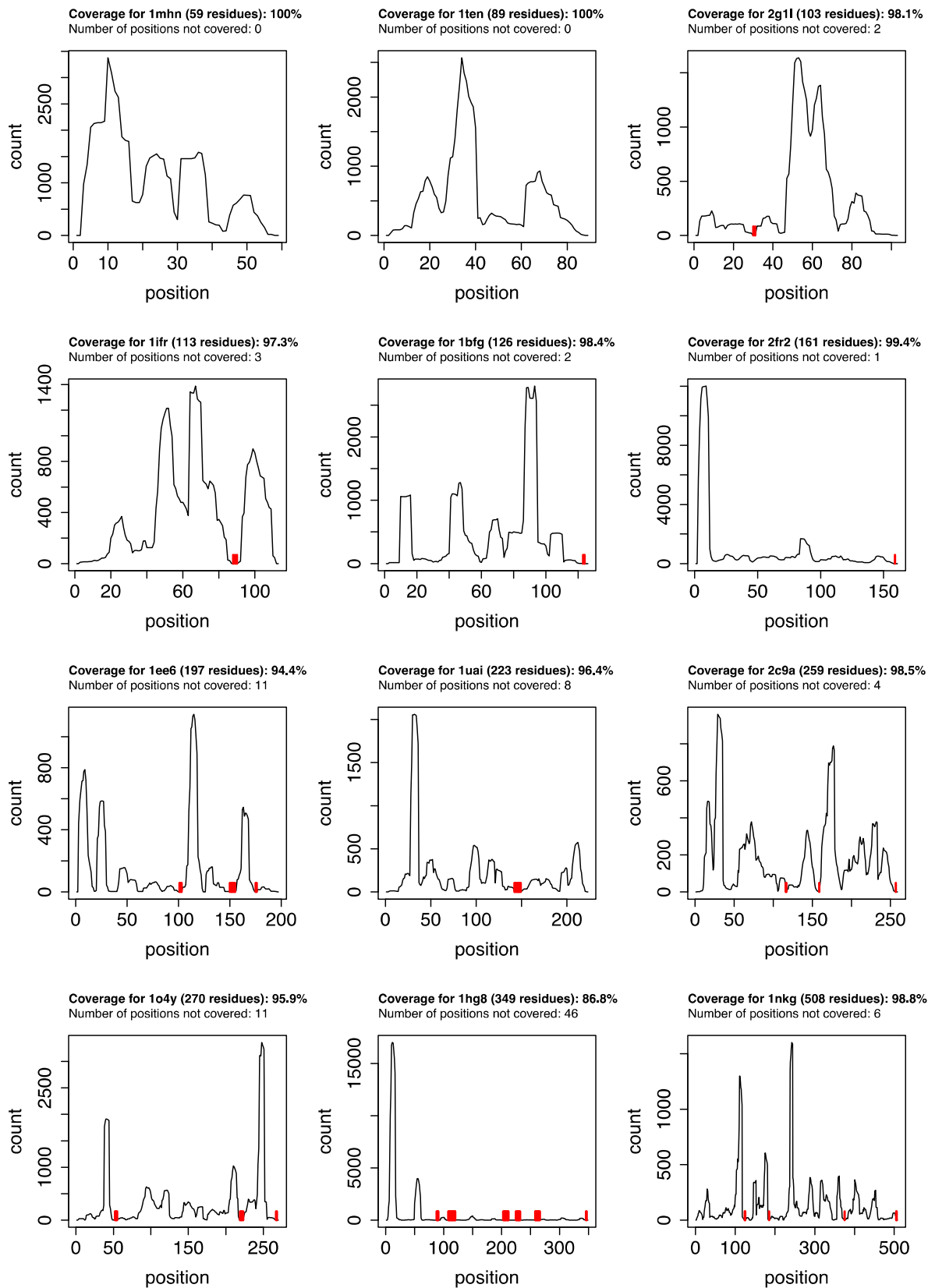
Supplementary Figure 1.1a

Protein Block Assignment (PBA) - SCOP Class – all α



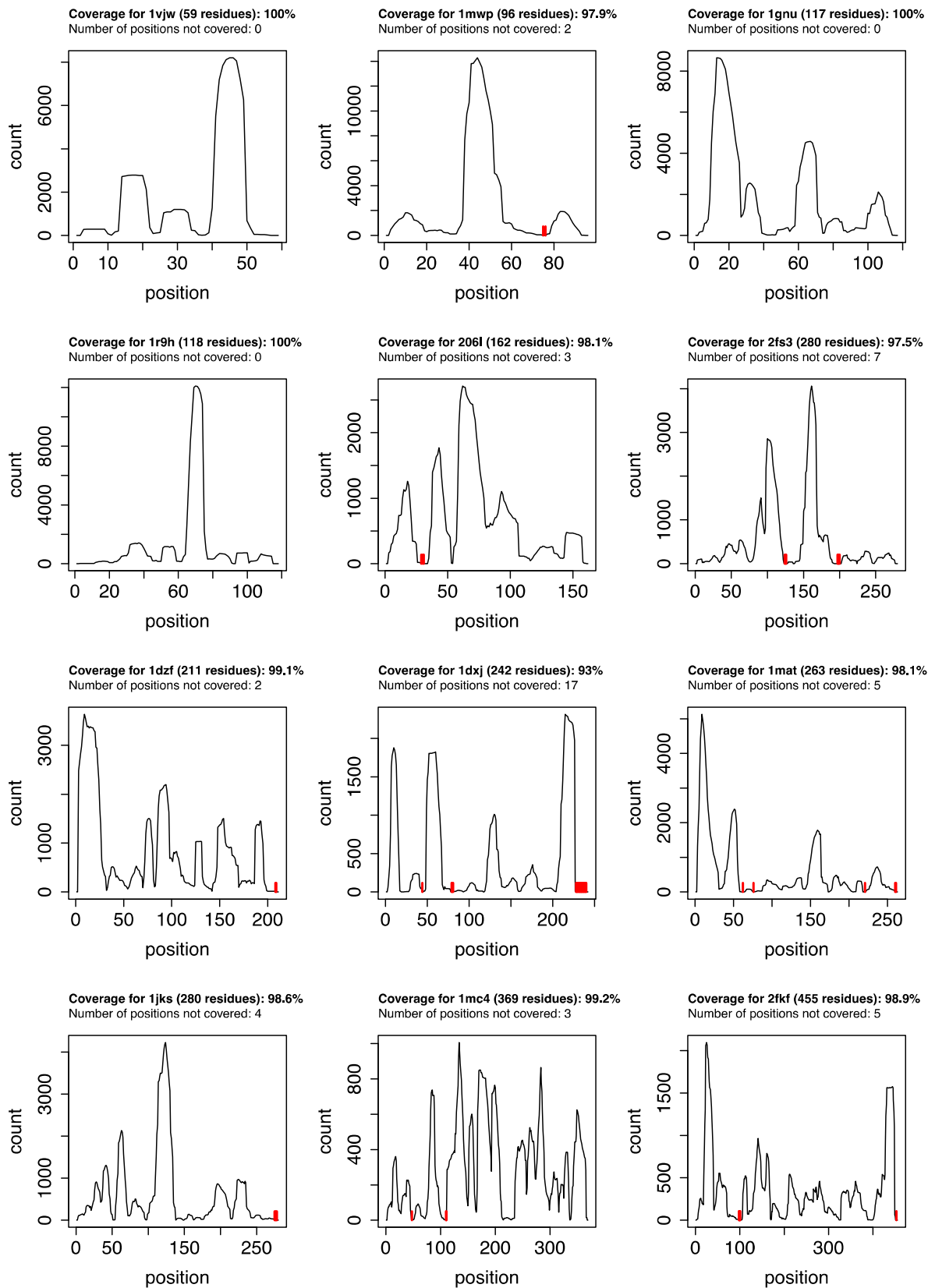
Supplementary Figure 1.1b

Protein Block Assignment (PBA) – SCOP Class – all β



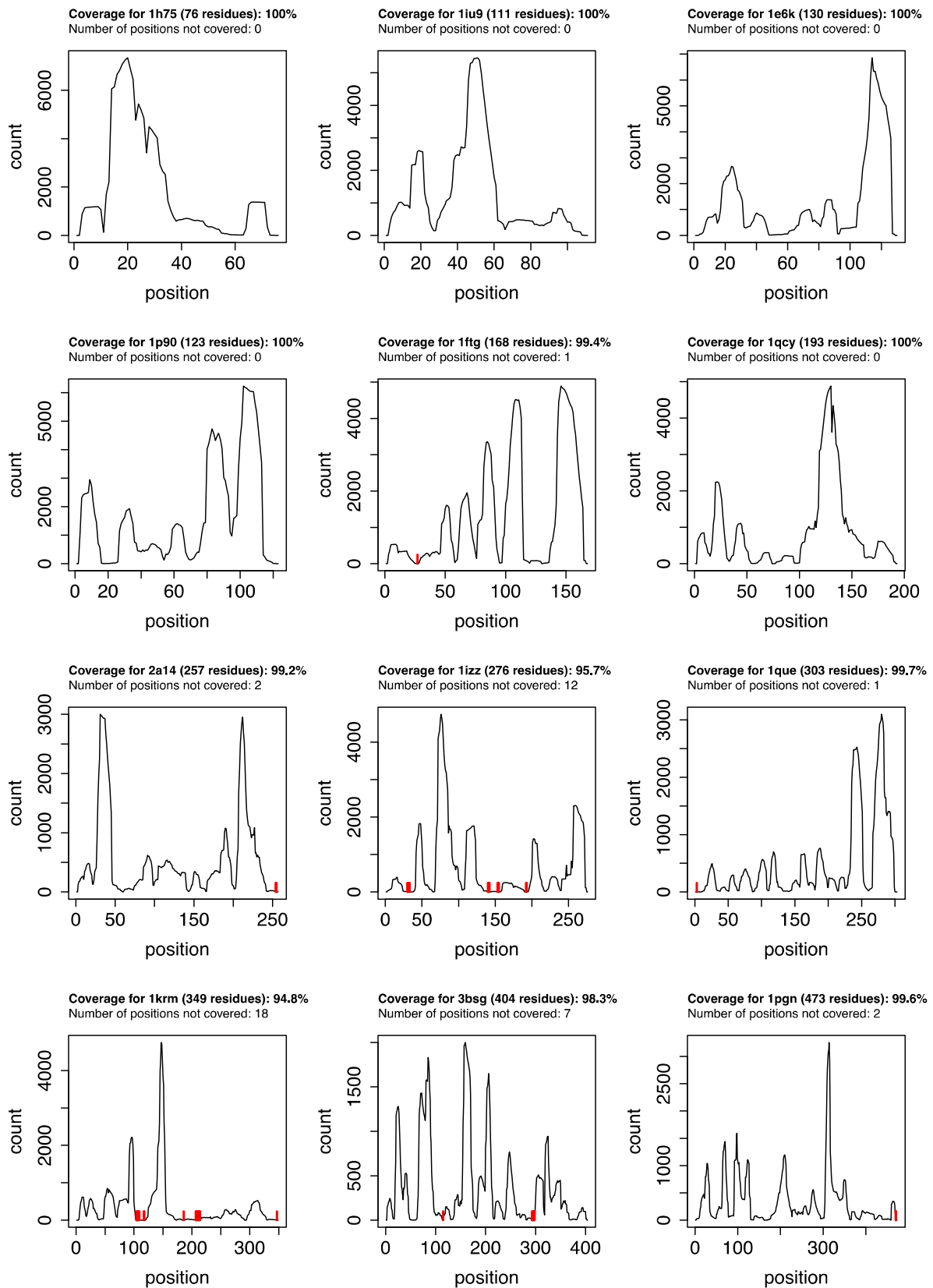
Supplementary Figure 1.1c

Protein Block Assignment (PBA) – SCOP Class – $\alpha+\beta$



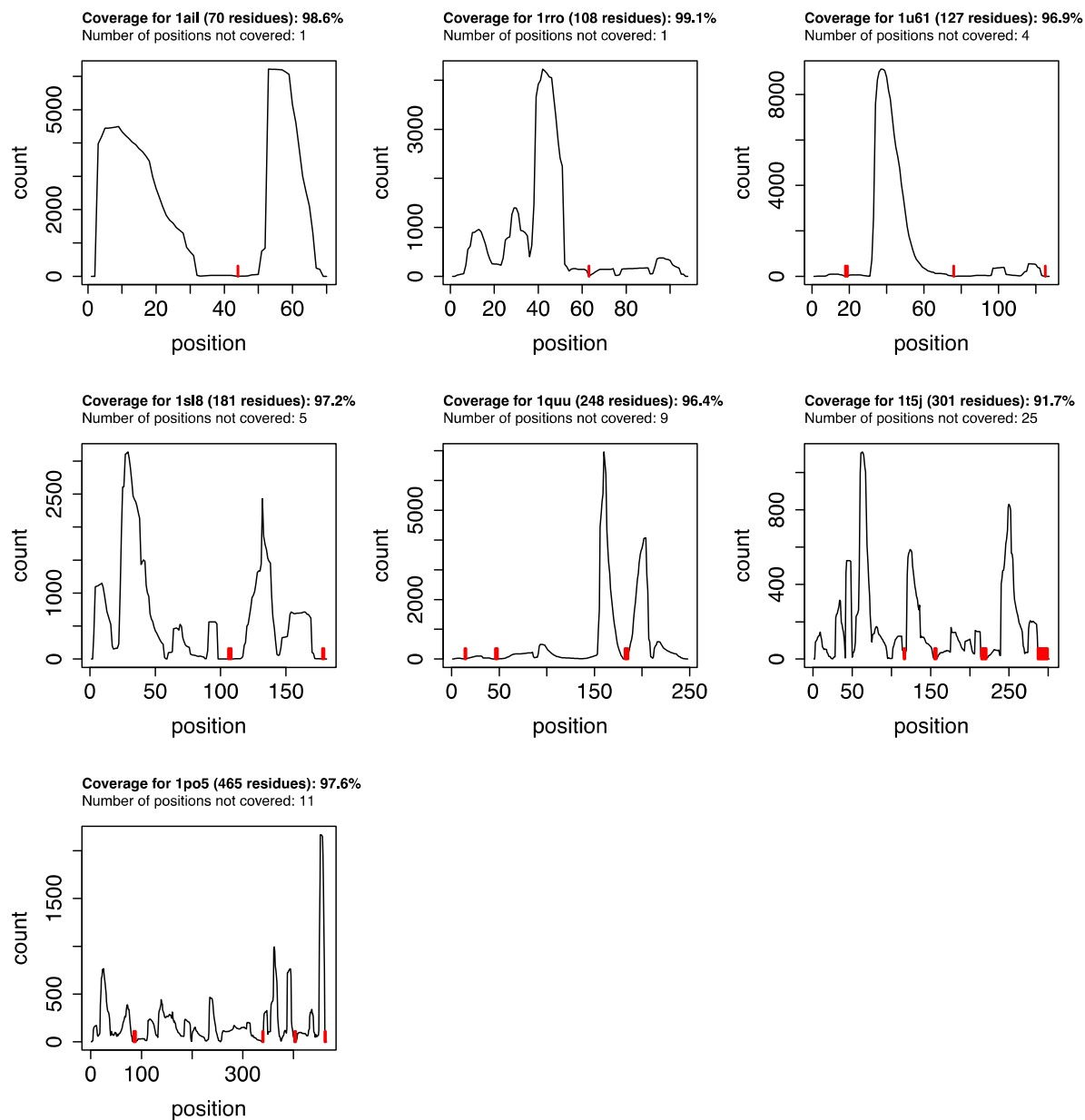
Supplementary Figure 1.1d

Protein Block Assignment (PBA) – SCOP Class – α/β



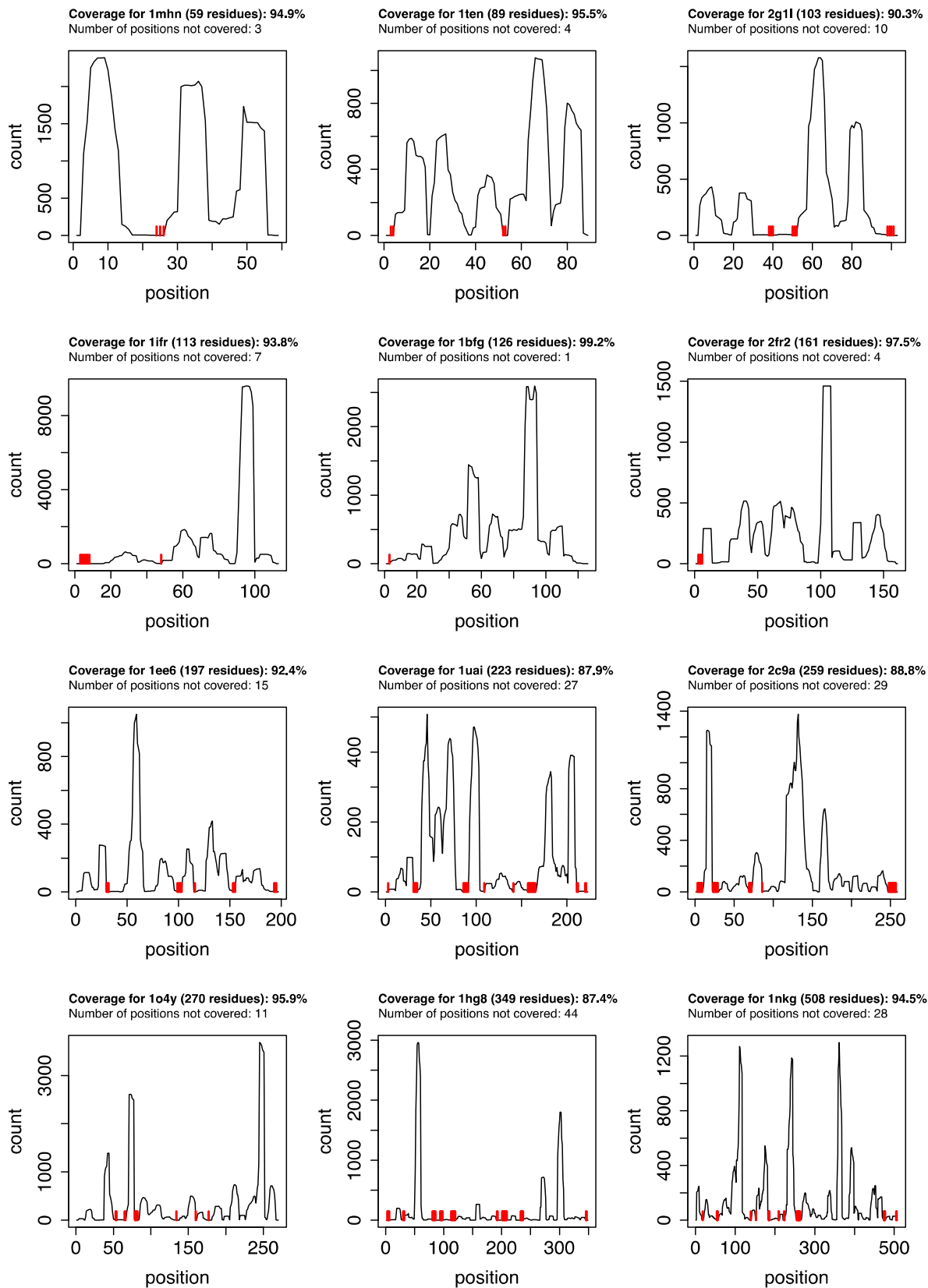
Supplementary Figure 1.2a

Protein Block Prediction (PBP) - SCOP Class – all α



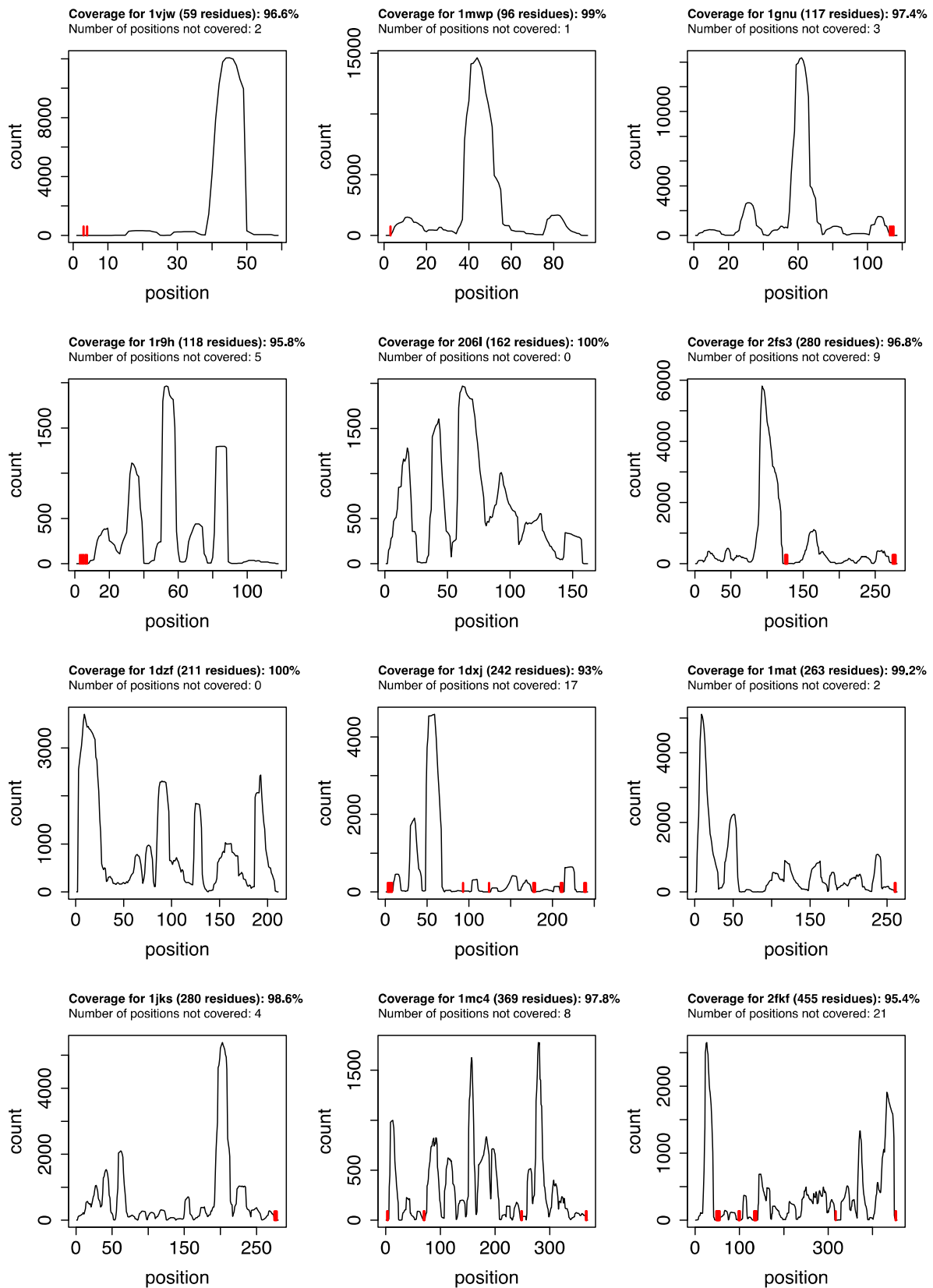
Supplementary Figure 1.2b

Protein Block Prediction (PBP) - SCOP Class – all β



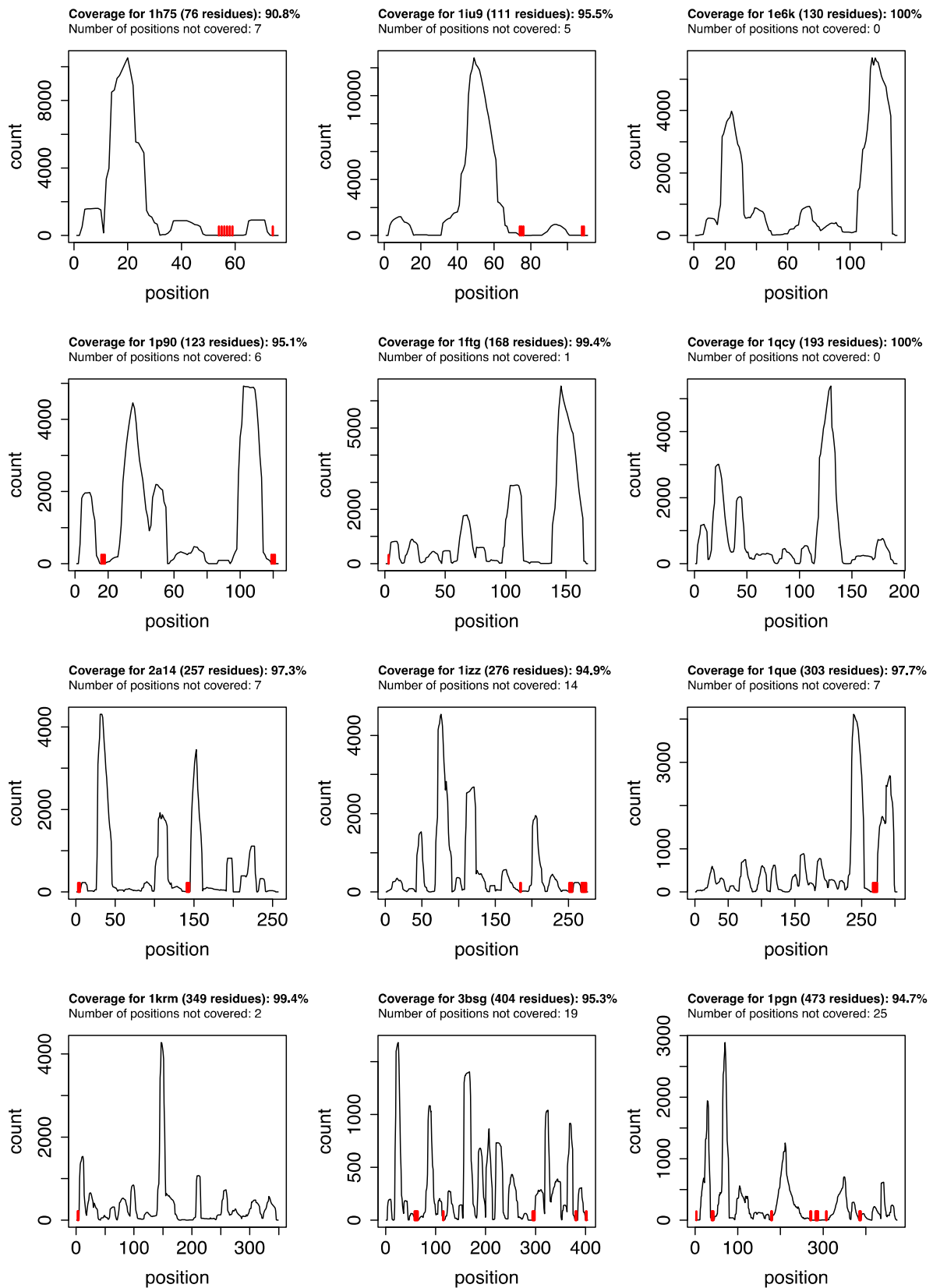
Supplementary Figure 1.2c

Protein Block Prediction (PBP) - SCOP Class – $\alpha+\beta$



Supplementary Figure 1.2d

Protein Block Prediction (PBP) - SCOP Class – α/β

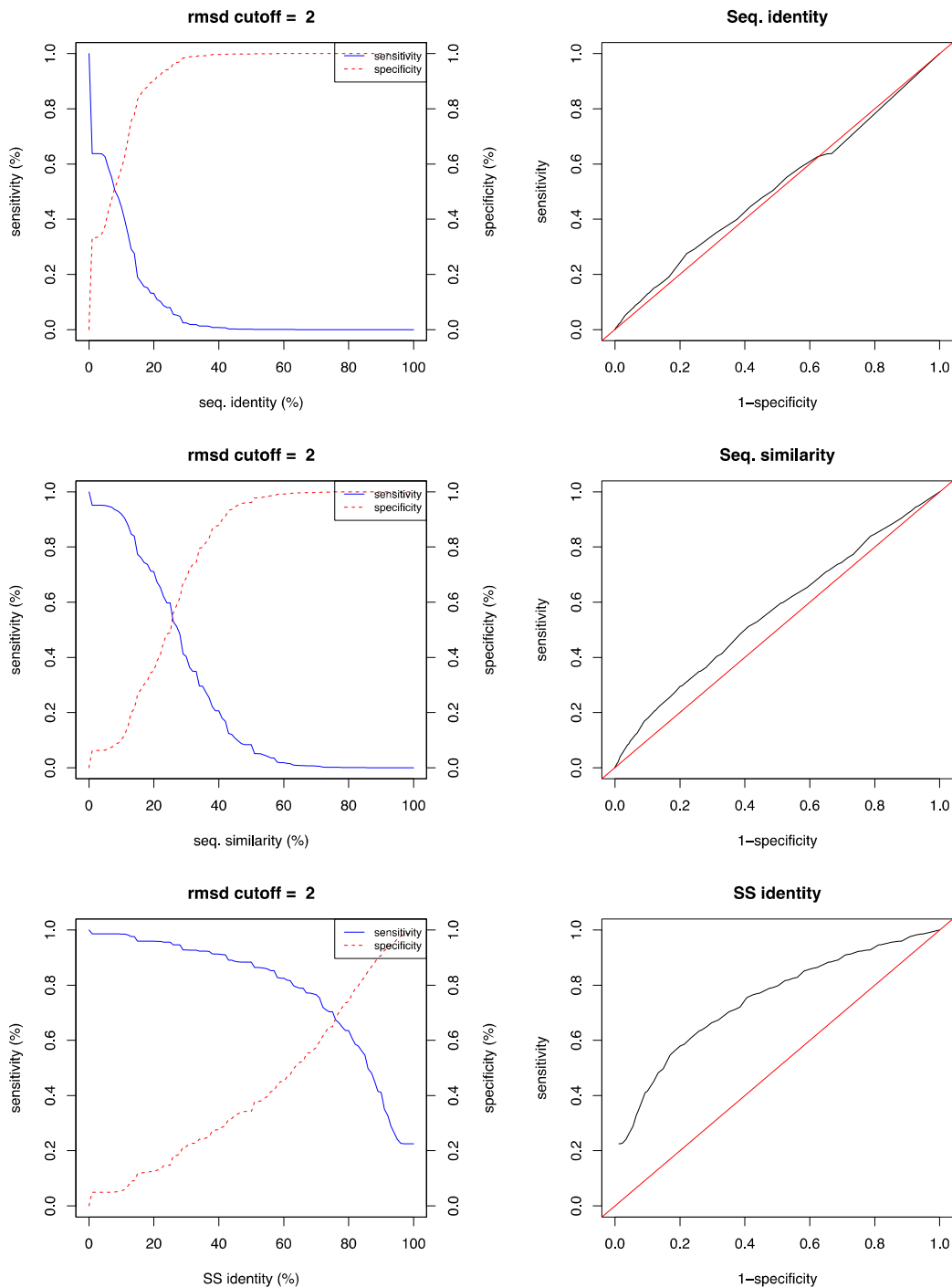


Supplementary Figures 2. Sensitivity and specificity Plots.

The plots under this heading show the co-relation between *rmsd* (2 Å) and three chosen criteria for prioritizing fragment selection, i.e., protein sequence identity, protein sequence similarity and secondary structure identity. The analysis has been performed for both treatment of the query proteins: (1) Protein Block Assignment (PBA) and (2) Protein Block Prediction (PBP). The graphs are further classified into section : (a) SCOP Class –all α , (b) SCOP Class – all β , (c) SCOP Class - $\alpha+\beta$ and (d) SCOP Class - α/β .

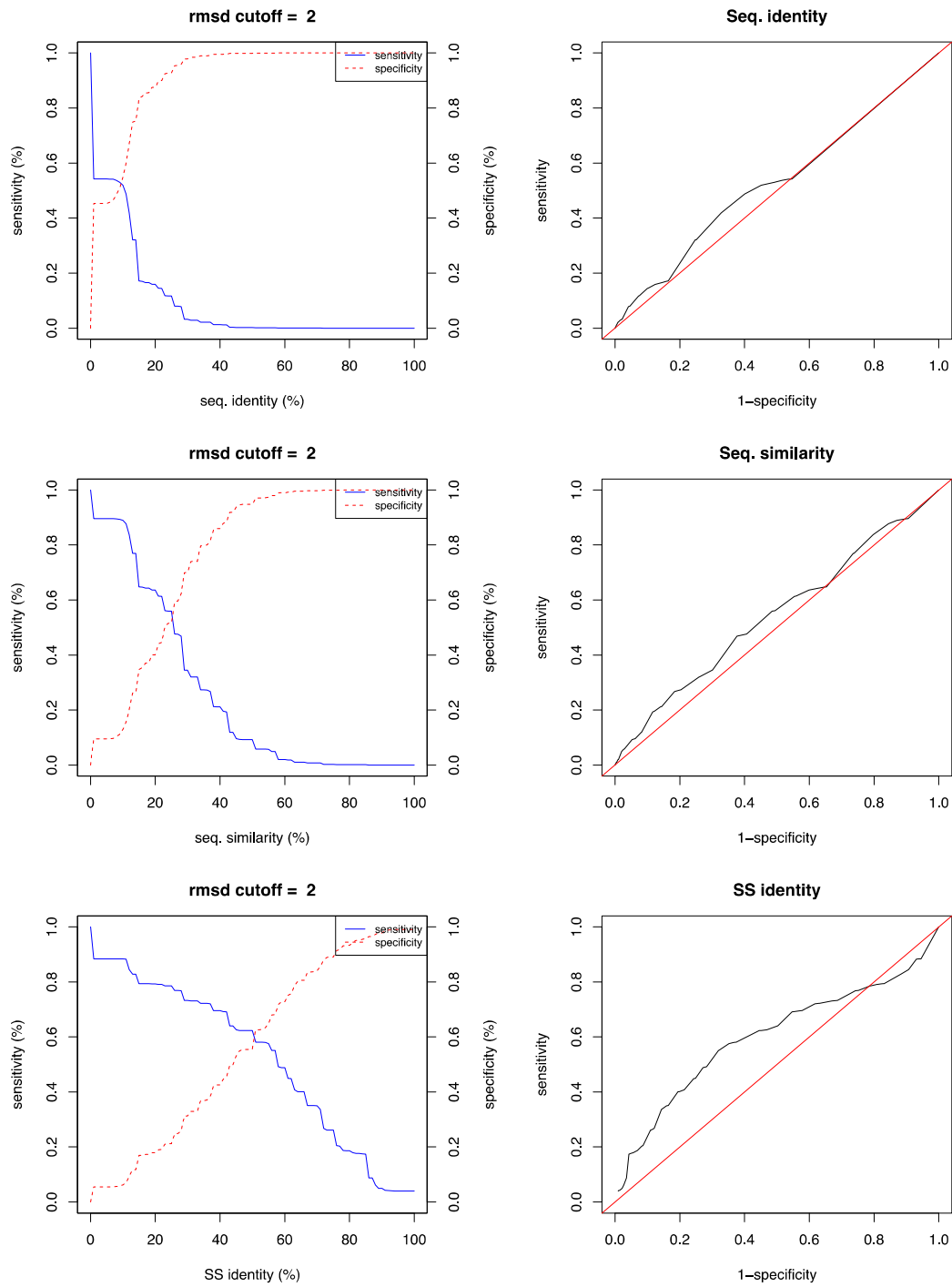
Supplementary Figure 2.1a

Protein Block Assignment (PBA) - SCOP Class – all α



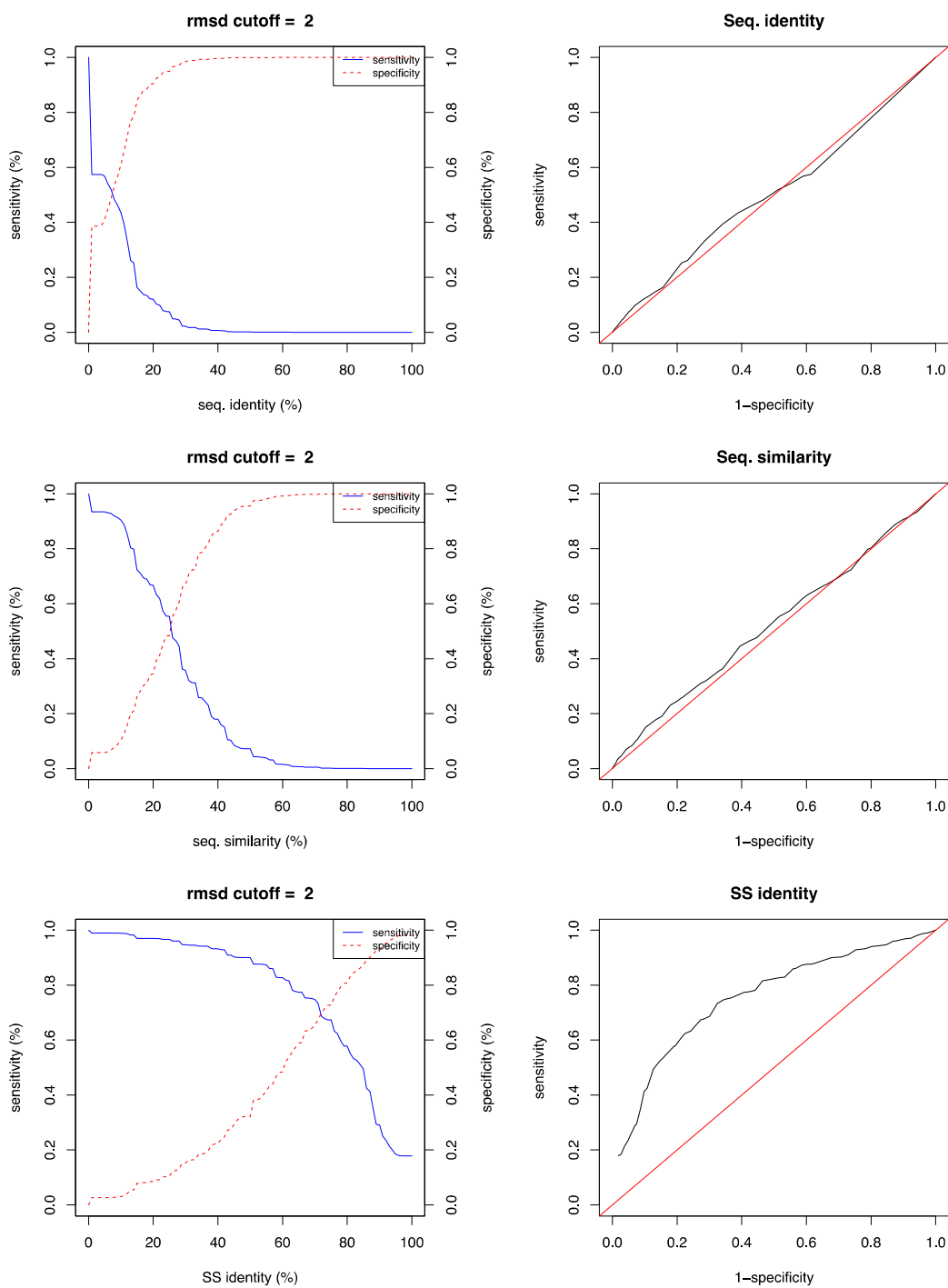
Supplementary Figure 2.1b

Protein Block Assignment (PBA) – SCOP Class – all β



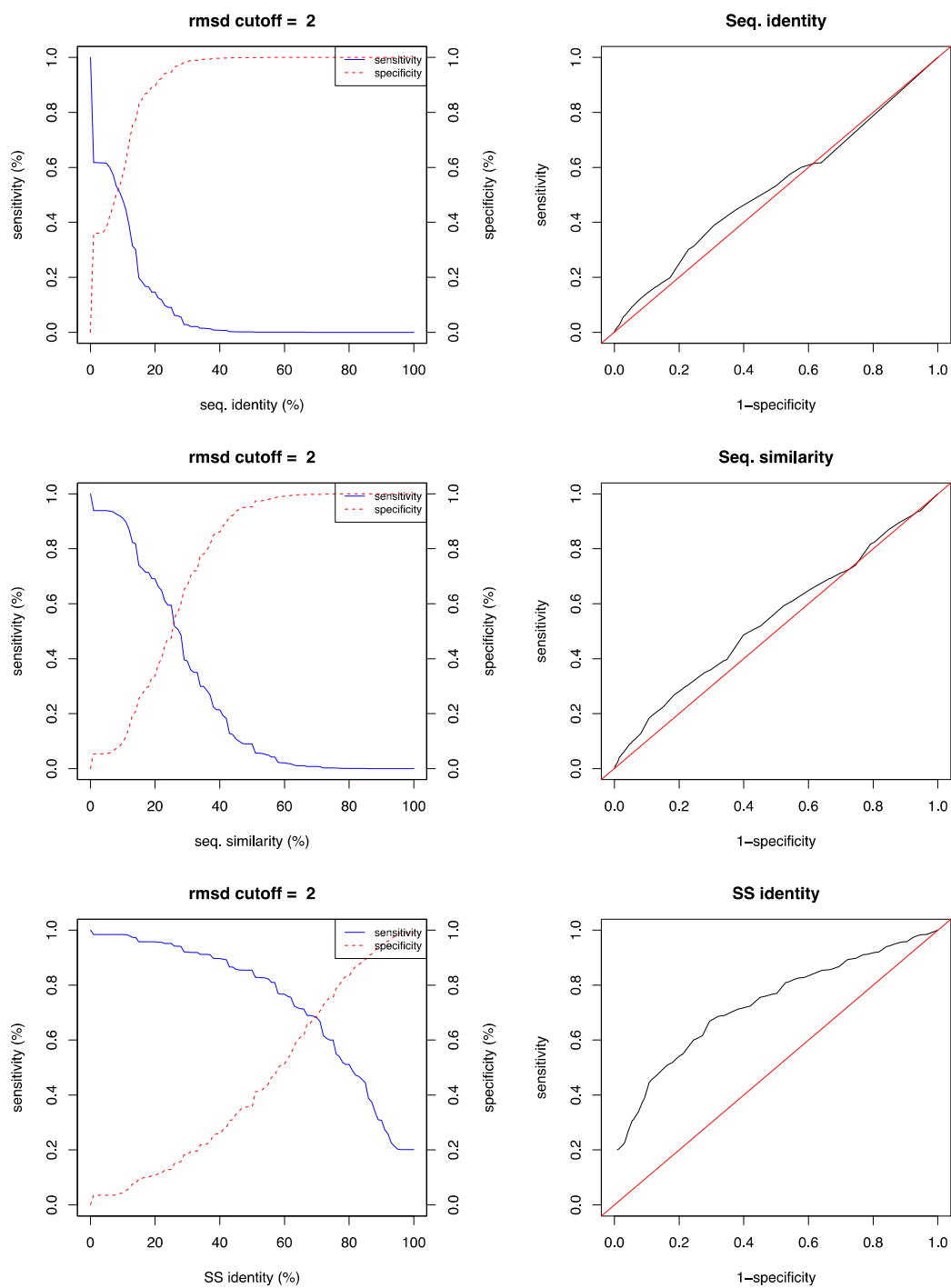
Supplementary Figure 2.1c

Protein Block Assignment (PBA) – SCOP Class – $\alpha+\beta$



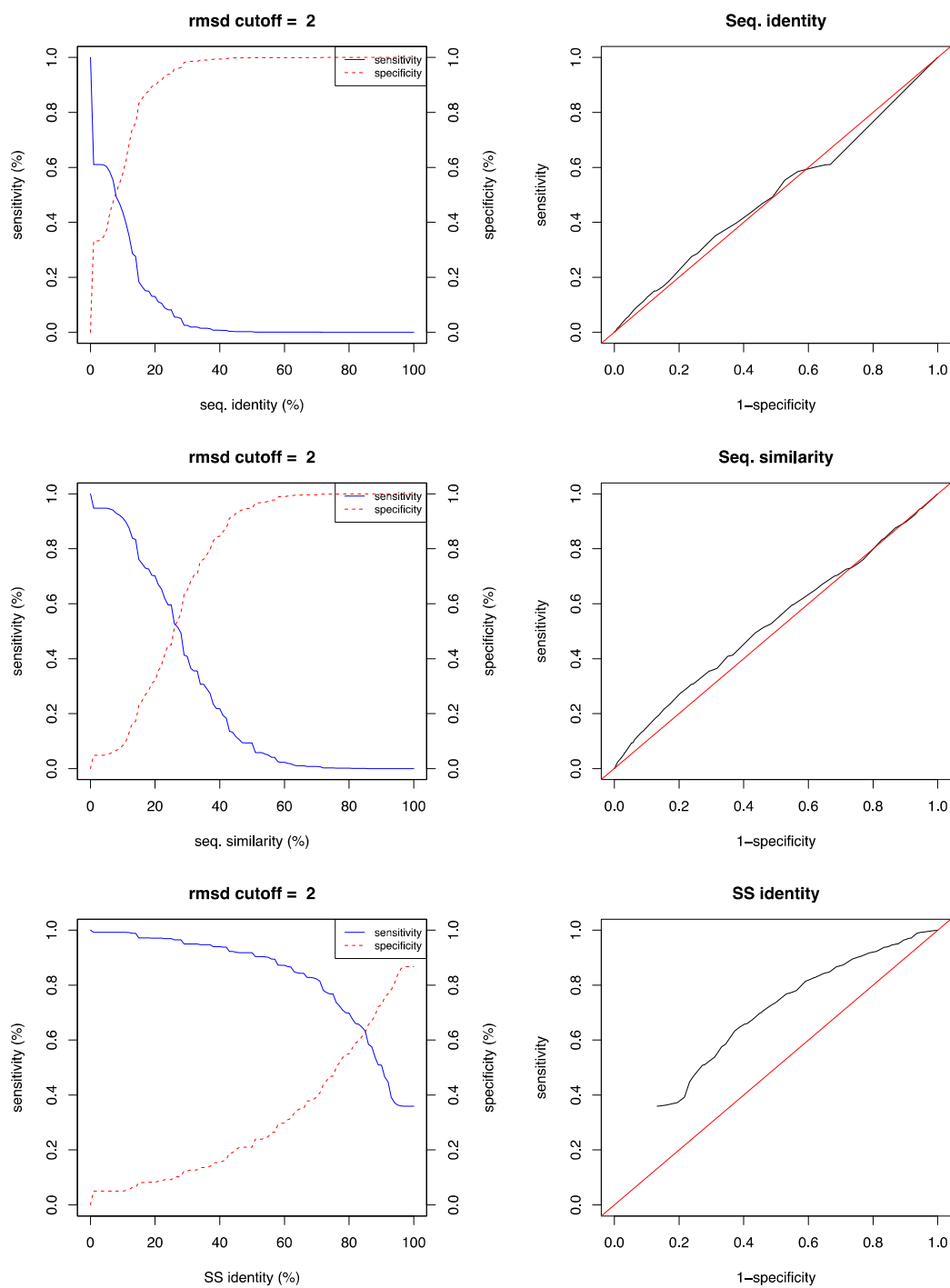
Supplementary Figure 2.1d

Protein Block Assignment (PBA) – SCOP Class – α/β



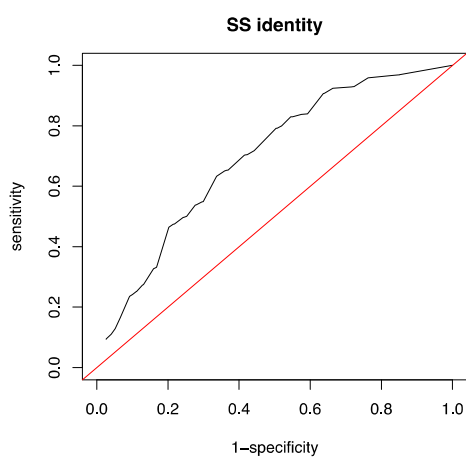
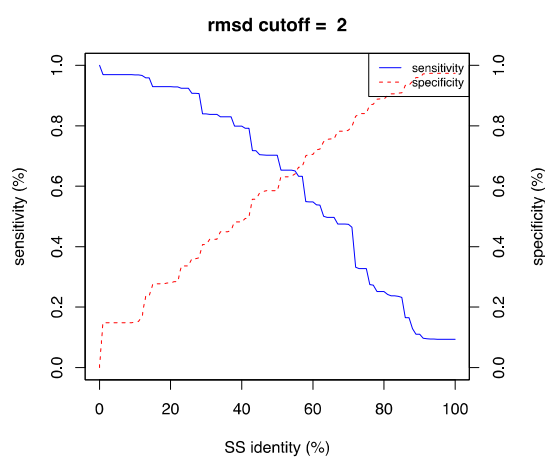
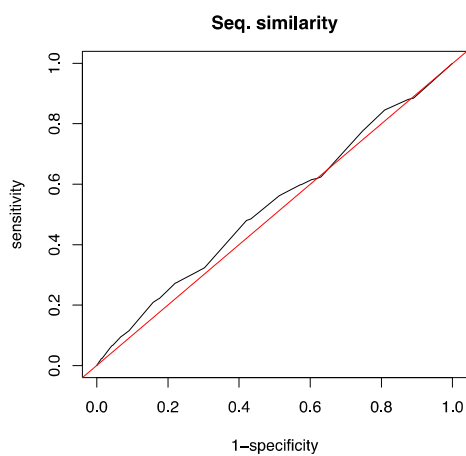
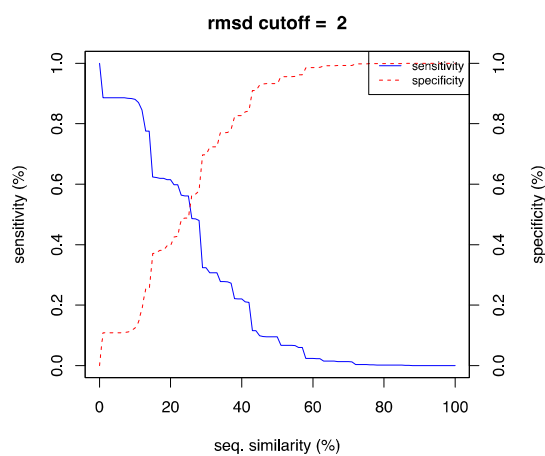
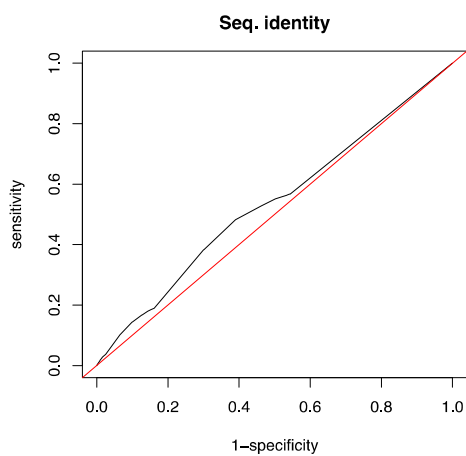
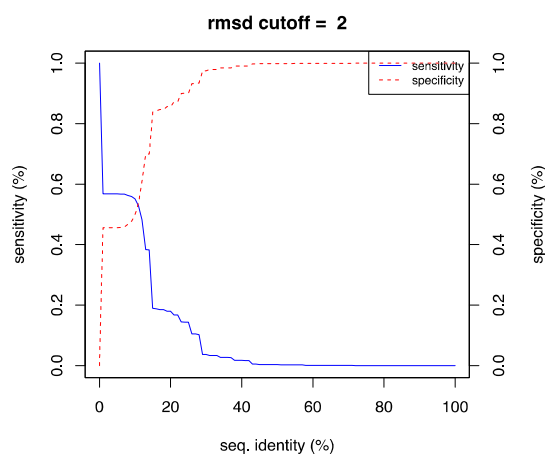
Supplementary Figure 2.2a

Protein Block Prediction (PBP) - SCOP Class – all α



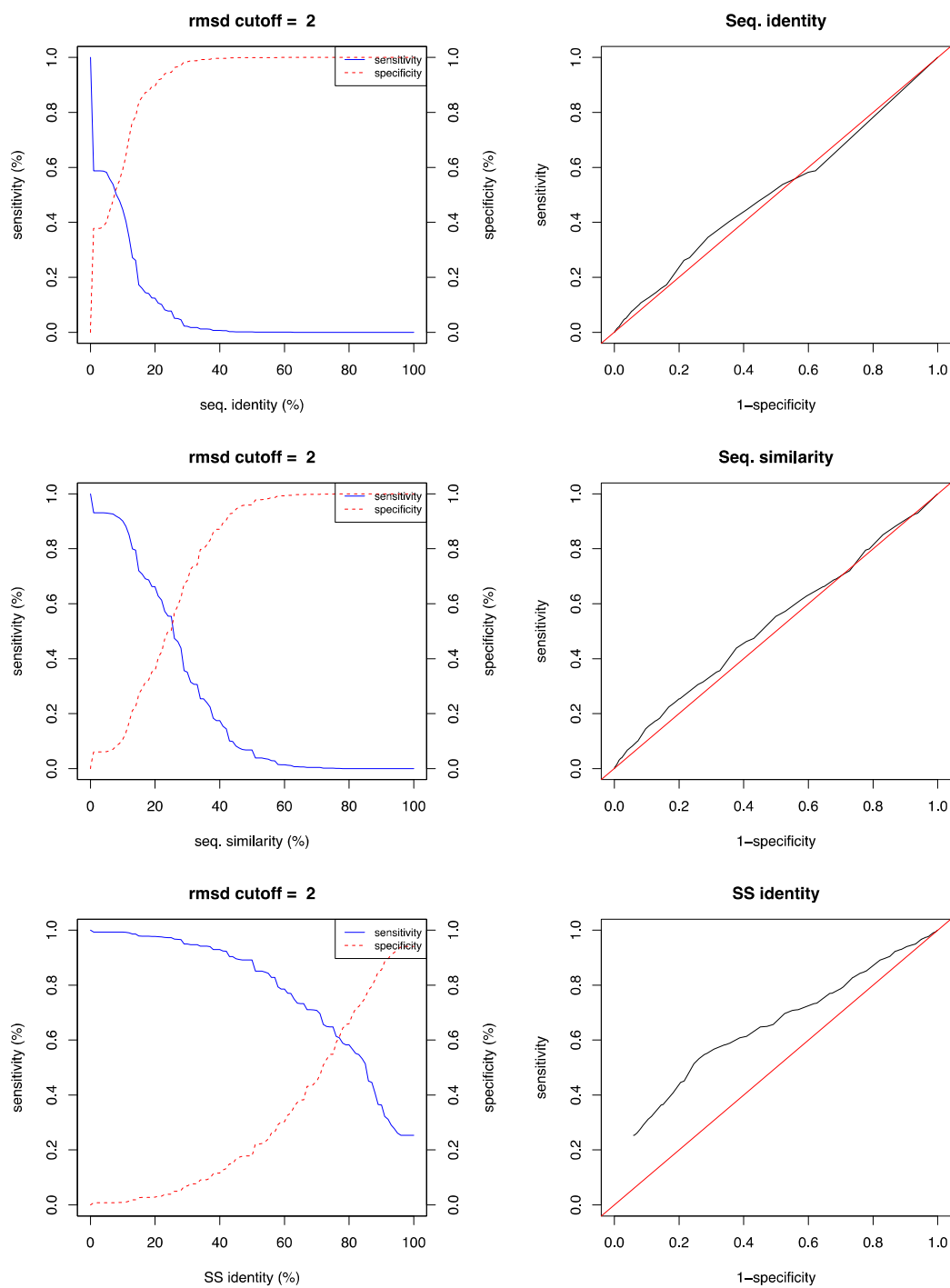
Supplementary Figure 2.2b

Protein Block Prediction (PBP) - SCOP Class – all β



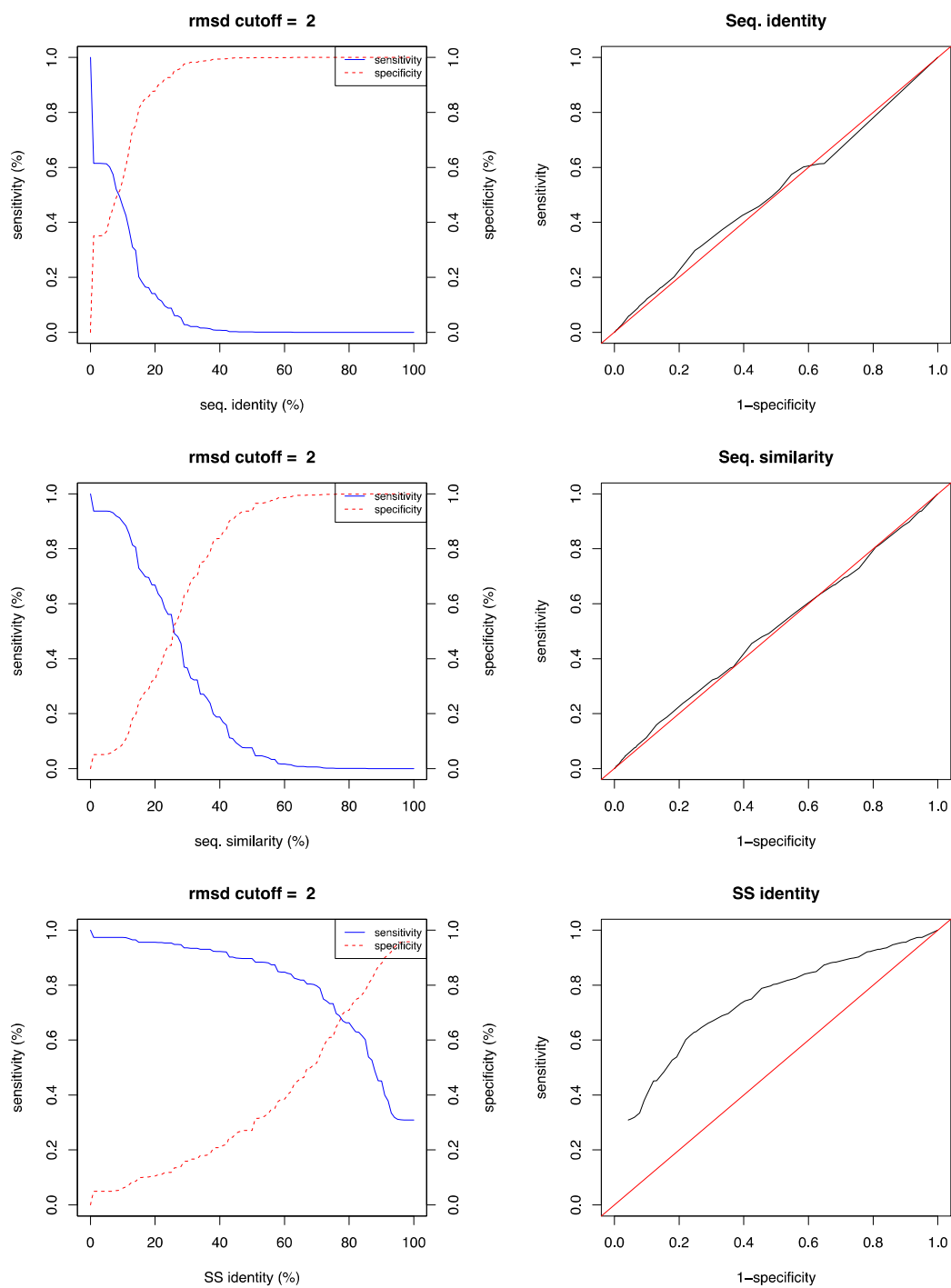
Supplementary Figure 2.2c

Protein Block Prediction (PBP) - SCOP Class – $\alpha+\beta$



Supplementary Figure 2.2d

Protein Block Prediction (PBP) - SCOP Class – α/β



Supplementary Table 1. This table provides the fragment hit counts obtained after Protein Block Assignment (PBA) for each protein from the query dataset.

PB Assignment

	PDB ID	Length (AA)	Length (PDB)	All Hits	Identical PB Hits	Longest Hits	Coverage (%)
All Alpha	1AIL	73	70	34655	14402	150	100
	1RRO	108	108	49734	9728	415	100
	1U61	138	127	38640	6490	358	100
	1SL8	191	181	44102	8195	402	98.9
	1QUU	250	248	44824	11293	225	100
	1T5J	313	301	51463	6480	658	100
	1PO5	476	465	63837	9992	1569	97.8
All Beta	1MHN	59	59	45693	7763	172	100
	1TEN	90	89	41975	5675	232	100
	2G1L	104	103	44320	4135	343	98.1
	1IFR	121	113	43452	5637	270	97.3
	1BFG	146	126	57287	7341	343	98.4
	2FR2	172	161	78928	18226	392	99.4
	1EE6	197	197	42734	3761	471	94.4
	1UAI	224	223	45133	5718	437	96.4
	2C9A	259	259	44350	5378	717	98.5
	1O4Y	288	270	63734	10210	791	95.9
	1HG8	349	349	86866	22834	505	86.8
	1NKG	508	508	55584	8251	1841	98.8
Alpha and Beta	1VJW	60	59	72137	12525	235	100
	1MWP	96	96	73965	21732	461	97.9
	1GNU	117	117	73953	19932	583	100
	1R9H	135	118	76827	17704	558	100
	206L	164	162	55886	9290	861	98.1
	2FS3	282	280	64493	13195	674	97.5
	1DZF	215	211	70425	15982	850	99.1
	1DXJ	242	242	59053	8455	791	93
	1MAT	264	263	62926	13142	1024	98.1
	1JKS	294	280	66566	13929	885	98.6
	1MC4	370	369	61250	9888	739	99.2
2FKF	462	455	61147	13037	1300	98.9	
Alpha/Beta	1H75	81	76	69484	13346	299	100
	1IU9	111	111	66589	13346	342	100
	1E6K	130	130	71746	16321	621	100
	1P90	145	123	73913	20568	363	100
	1FTG	168	168	72925	18987	711	99.4
	1QCY	193	193	69619	15430	532	100
	2A14	263	257	64677	12697	835	99.2
	1ZZ	283	276	71107	16494	770	95.7
	1QUE	303	303	62765	12752	742	99.7
	1KRM	356	349	67668	12602	779	94.8
	3BSG	414	404	67000	14272	832	98.3
1PGN	482	473	66032	14479	1019	99.6	

Supplementary Table 2. This table provides the fragment hit counts obtained after Protein Block Prediction (PBP) for each protein from the query dataset.

PB Prediction

	PDB ID	Length (AA)	Length (PDB)	All Hits	Identical PB Hits	Longest Hits	Coverage (%)
All Alpha	1AIL	73	70	38447	11501	414	98.6
	1RRO	108	108	40842	7661	451	99.1
	1U61	138	127	56844	10419	248	96.9
	1SL8	191	181	50381	10150	984	97.2
	1QUU	250	248	53552	12696	441	96.4
	1T5J	313	301	54456	4973	668	91.7
	1PO5	476	465	62554	9430	1591	97.6
All Beta	1MHN	59	59	70551	6379	380	94.9
	1TEN	90	90	69989	3775	859	95.5
	2G1L	104	103	45732	3721	317	90.3
	1IFR	121	113	66507	15170	946	93.8
	1BFG	146	126	53359	7121	482	99.2
	2FR2	172	161	60031	4934	2542	97.5
	1EE6	197	197	49351	3073	792	92.4
	1UAI	224	223	47480	2926	740	87.9
	2C9A	259	259	59190	5551	705	88.8
	1O4Y	288	270	67912	12023	1869	95.9
	1HG8	349	349	50990	6720	659	87.4
	1NKG	508	508	56424	8486	1530	94.5
	Alpha+Beta	1VJW	60	59	61326	12716	157
1MWP		96	96	73836	21621	308	99
1GNU		117	117	82325	21173	780	97.4
1R9H		135	118	51549	5452	636	95.8
206L		164	162	53082	8458	736	100
2FS3		282	280	64098	12754	1236	96.8
1DZF		215	211	70028	17204	824	100
1DXJ		242	242	63698	9378	500	93
1MAT		264	263	63583	13768	909	99.2
1JKS		294	280	69244	16160	1134	98.6
1MC4		370	369	66492	11564	1209	97.8
2FKF		462	455	64106	14040	1236	95.4
Alpha/Beta	1H75	81	76	72386	14483	729	90.8
	1IU9	111	111	66329	18860	1258	95.5
	1E6K	130	130	72078	15837	1205	100
	1P90	145	123	74454	15671	2383	95.1
	1FTG	168	168	70585	14923	587	99.4
	1QCY	193	193	69674	15537	687	100
	2A14	263	257	66681	14408	2781	97.3
	1IZZ	283	276	71995	14779	1563	94.9
	1QUE	303	303	64904	14981	889	97.7
	1KRM	356	349	67838	13370	605	99.4
	3BSG	414	404	67614	11980	1006	95.3
1PGN	482	473	65827	11766	1414	94.7	